

LAPPEENRANTA UNIVERSITY OF TECHNOLOGY

Lappeenranta School of Engineering Science

Technical Physics

Kirill Potapov

ANTENNA FEED DESIGN FOR OMNIDIRECTIONAL BROADBAND ANTENNA

Examiners: Professor Andrey Cherepanov

Professor ErkkiLähderanta

ABSTRACT

LAPPEENRANTA UNIVERSITY OF TECHNOLOGY

Lappeenranta School of Engineering Science

Technical Physics

Kirill Potapov

Antenna feed design for omnidirectional broadband antenna

Master's thesis

2015

Pages, figures and tables

Scientific directors: Professor Andrey Cherepanov

Professor Erkki Lähderanta

Keywords: development, feed, "eleven" antenna, quad ridged horn, polarization, phase center, coupler, radiation pattern, VSWR

This thesis is about development broadband feed for two-mirror antenna system that match following requirements: beamwidth from 45° to 90° at -3 dB level, circular polarization, absence of radiation to the lower hemisphere area. Literature review was done in the areas of the UWB antennas creation. During the work attempts were made to create a feed in a form of the quad ridged horn and "eleven" antennas. The latter is introduced as the most effective feed among all antennas discussed in thesis. Radiation patterns and other results for "eleven" antenna were obtained. Results were saved as far field sources and placed slightly below focal point into the two-mirror antenna system, because phase center of the "eleven" antenna is predominantly shifted upwards. Directivity patterns for the two-mirror system were obtained and the conclusions about the work results have been made.

ACKNOWLEDGEMENTS

Work was done in the research institute “VECTOR”, located in Saint Petersburg.

Part of this work was done in the collaboration with Surikov Vladimir Vasilievich.

I would like to express my grate gratitude to my scientific director in Polytechnical University Cherepanov Andrey Sergeevich, who supported my choice to work away from university, and supported me during my work there.

I would like to express my appreciations and thanks to my LUT supervisor Professor Erkki Lähderanta for great time I spent during my study in LUT University.

I would like to express my gratitude to the Lappeentanta University of Technology for the possibility to graduate from Finnish University and financial support during my studies.

I wish to thank my mother and my girlfriend Natasha for their love and support.

Lappeentanta, 2015

Kirill Potapov

CONTENTS

ABSTRACT.....	2
ACKNOWLEDGEMENTS.....	3
List of abbreviations.....	5
INTRODUCTION.....	6
1 LITERATURE REVIEW AND SELECTION OF THE IRRADIATOR DESIGN.....	8
2 QUAD RIDGED HORN ANTENNA.....	12
2.1 Modelling the horn.....	12
2.2 Results of modelling and optimization.....	16
2.3 Conclusions.....	22
3 “ELEVEN” ANTENNA.....	23
3.1 Modelling the irradiator in the form of “eleven” antenna.....	23
3.2 Results of modelling and optimization.....	27
4 TWO-MIRROR ANTENNA SYSTEM.....	37
5 CONCLUSIONS.....	39
Bibliography.....	40

List of abbreviations

<i>VSWR</i>	voltage standing wave ratio
<i>UWB</i>	ultra wide band
<i>QRHA</i>	quad ridged horn antenna
<i>AR</i>	axial ratio

INTRODUCTION

In the development of modern systems of radio monitoring appears a steady trend of the widening of the frequency range. Currently this is achieved by changing blocks of antenna systems. Great problems of their usage are also related to this. Herewith, to locate low energy objects, and for the increasing range of locations, usage of antenna systems with high gain is needed. Therefore, people are trying to create broadband antenna systems with high gain.

Purpose of this work is development of the feed, irradiator, for the broadband omnidirectional (in the azimuth plane) antenna system, that is made on the two-mirror scheme basis for radio monitoring purposes. The design of this system is presented on the fig. 1.1.

Requirements for the radiator are the following:

- 1) Frequency range 2-16 GHz
- 2) Beamwidth (-3dB level) from 45° to 90°
- 3) Circular polarization
- 4) Ellipticity at maximum ≤ 3 dB
- 5) Minimum (≤ -15 dB) backward radiation, for lowering the side lobes level

Presently, spiral antenna is used as the feed for the antenna system; its characteristics is presented below. However, it has very low gain (≤ 4 dB) over almost entire frequency band. Therefore, the necessity of creating high-gain antenna occurred. During the research, two types of antennas were studied: ridged horn antenna and log-periodic “eleven” antenna. Both combine properties of orthogonal and linear polarization and ultra-wideband frequency range.

Antennas, that are presented, were modelled in the CST Microwave Studio program, in the frequency range of 2-16 GHz. Optimization of antenna constructions was done to lower VSWR (voltage standing wave ratio) and to obtain acceptable directivity patterns for all frequency range. Results of the intermediate steps of the work were fixed and also presented in this paper. Later the construction based on the quad ridged horn was given up, due to phase center instability and presence of the backward radiation at low frequencies. The choice was made for the “eleven” antenna, because for it acceptable results were obtained. Later on, the directivity pattern of the feed (“eleven” antenna) was placed to the model of two-mirror antenna system, as the Farfield source. Results that met the requirements were obtained for it that led to the future

work of creating the physical model. Conclusions and comparisons with results, obtained using the spiral antenna as the feed for antenna system were made. Modelling progress and its results, such as VSWR, gain, ellipticity, directivity patterns for different frequencies, intermediate results of the optimization are also presented in this work.

Some scientific results, obtained from this work are the following:

- 1) For the ridged horn, it was obtained that the profile of the ridges influences the radiation properties. Usage of any function without any further optimization for its creation is not acceptable for getting appropriate results.
- 2) For “eleven” antenna, it was obtained that the design of its feed part and the number of log-periodic elements has very significant impact on its matching (VSWR).

Practical significance of the results of the research lies in the fact that the proposed structure of the radiator for two-mirror scheme system has several advantages over existing, and can serve as the basis for modern radio monitoring systems.

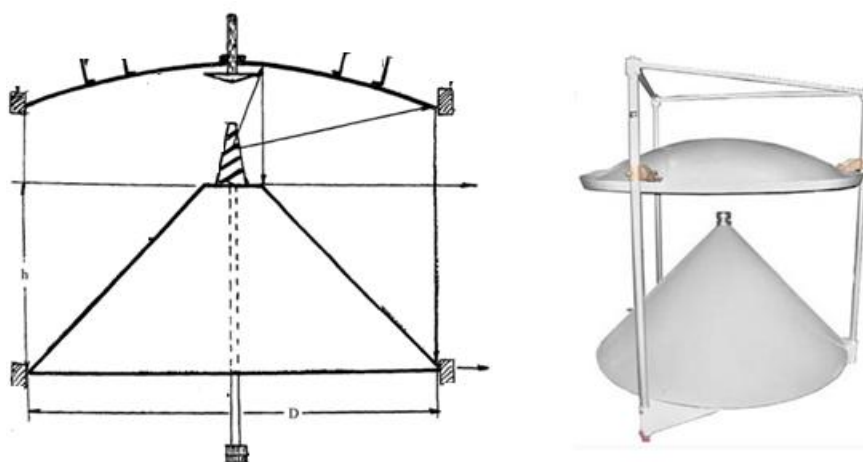


Fig. 1.1 Construction of two-mirror antenna system.

1 LITERATURE REVIEW AND SELECTION OF THE IRRADIATOR DESIGN

Electrical properties of antennas capable to receive or transmit a signal in the range of frequencies 1:10, i.e. the characteristic of radiation, gain and matching with feed line, either should remain constant, or vary within allowable limits, or possess an optimal frequency dependence. Along with the practical necessity to create such antennas with increased bandwidth, the question about the possibility of construction of so called “frequency independent” antennas has the scientific interest. While implementing broadband antennas other requirements must be met, particularly regarding side lobe levels.

Using antennas with circular (or elliptical) polarization in radiolocation technology allows to successfully suppress obstructive signals reflected from the homogeneous objects, such as signals from rain. Meanwhile, circular polarization is required for receiving any linearly polarized radiation.

If antenna dimensions increase or decrease, proportional to the wavelength, then its electrical properties are not changed. If the absolute size of antenna is not comparable with wavelength, it is obvious that its properties will not depend on frequency. Such antenna is identical to its increased or decreased model. Frequency range, used for real antennas, is mainly limited by the following:

- 1) For the long waves the size of the entire antenna. Approximate practical limit is the wavelength, and the maximum size of antenna is $\lambda/2$.
- 2) For short waves the dimensions of the feed junction. With decreasing of the wavelength, high order wave types occur, affecting both the radiation and matching. [1]

Thus, modelling antennas with increased bandwidth, dimension limits are considered from the beginning. Antenna can be designed so that the frequency dependence has periodicity at some extent. If, in this case, electrical properties could be retained constant (or nearly constant) for one period, this consistency can be achieved in the whole frequency range.

To design broadband antennas that are used for communications, radiolocation and for any application where it is needed to receive signals with a bandwidth wider than an octave, several basic types of structure are used. The main ones are: quad ridged horns [2]-[6], log-periodic [7]-[10] and spiral [11]. Such antennas are presented at fig. 1.2. below.

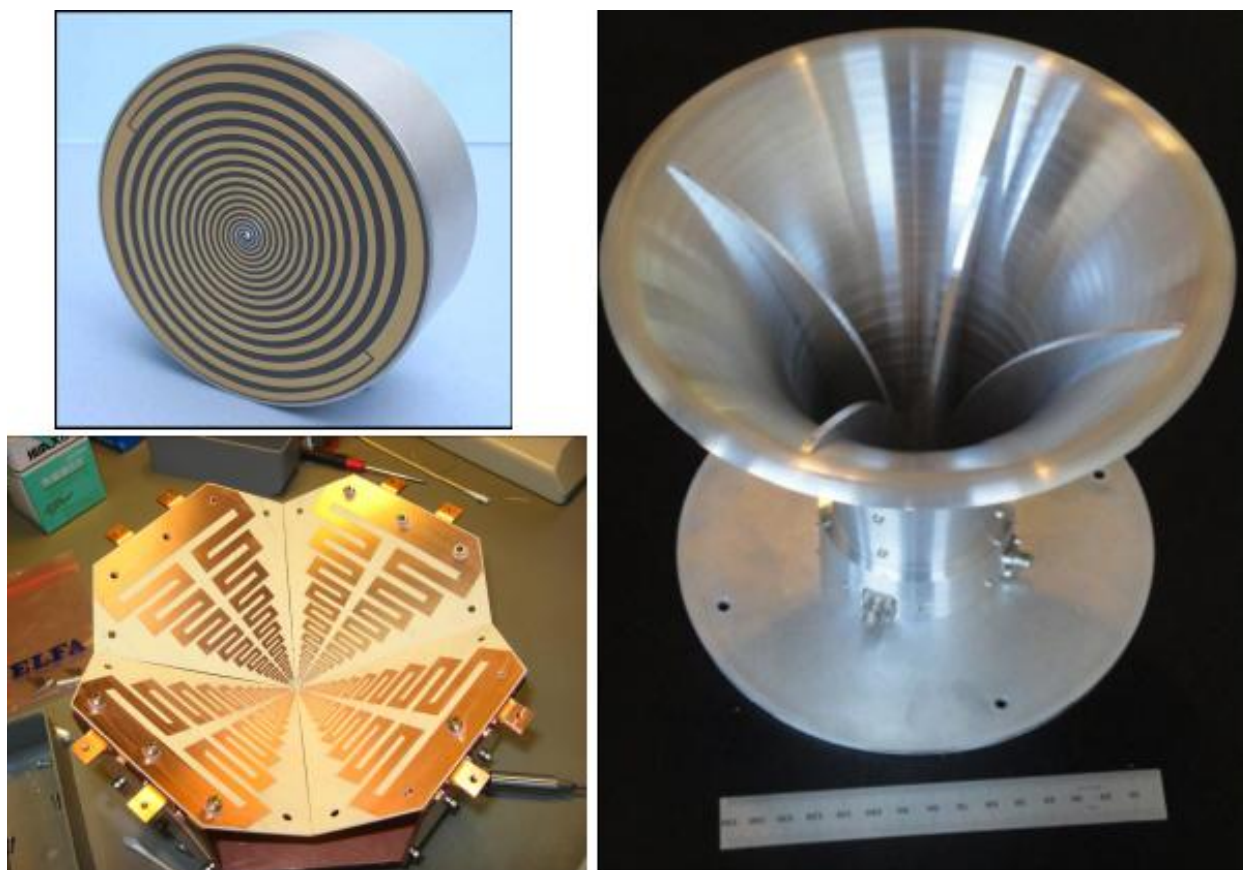


Fig. 1.2. Examples of the spiral antenna (top left), log-periodic “eleven” antenna (bottom left) and quad ridged horn (right).

Main advantage of ridged horns is the fact, that beamwidth could be varied from 30° to 120° (at -10 dB level), while changing the flare angle of ridges, and not changing the shape of entire horn. Feed point of such antennas is performed with minimum soldering, the input impedance is equal to 50-100 Ohms that allows a lossless matching with the coaxial cable. The gain of horn antennas is greater than for other broadband structures, though it is trade for quite narrow beamwidth in some cases. The main disadvantage of quad ridged horn as the radiator, is phase center and beamwidth deviation with frequency. However, there are investigations, where the stability of the directivity pattern and phase center was obtained [2].

Sinusoidal and self-complementary antennas are wideband log-periodic antennas of double polarization. The advantage of such antennas is the constant input impedance, equal to 188.5 Ohms. However, the ellipticity of the polarization of such antennas varies with frequency that is not suitable for solving the given task.



Fig. 1.3. Sinuous antenna (left) and self-complementary antenna (right).

The development of log-periodic UWB “eleven” antennas was performed during last years in “Chalmers University of Technology” (Gothenburg, Sweden). [7]-[9]. It was given that name due to the fact that it looks like two parallel bended half-wave dipoles. It can be used in the decade bandwidth, by logarithmic continuation of the basic design, with directive gain > 11 dBi. “Eleven” antenna can be used both for linear and circular polarization, deviation of its phase center with frequency is very small. Beamwidth (at -10 dB level) reaches $100-120^\circ$ at all frequency range. A lot of applications of “eleven” antennas as the irradiators for the reflectors of radio telescopes can be found in literature. The most known are Green Bank telescope (150-1700 MHz), RATAN (500-3000 MHz). Also “eleven” antenna was studied for usage in monopulse tracking systems.

Spiral antennas are also periodic. They stand out for phase center stability due to the fact that the spiral is located in one plane and the presence of the absorbent material between the coil and ground plane on the one side of the antenna. However, their gain is very small compared to the other UWB antennas. Fig. 1.5 represents the main characteristics of the spiral that is being used at the present time as the irradiator for the two-mirror system. In [11] full characteristics and directivity patterns are shown for that antenna.

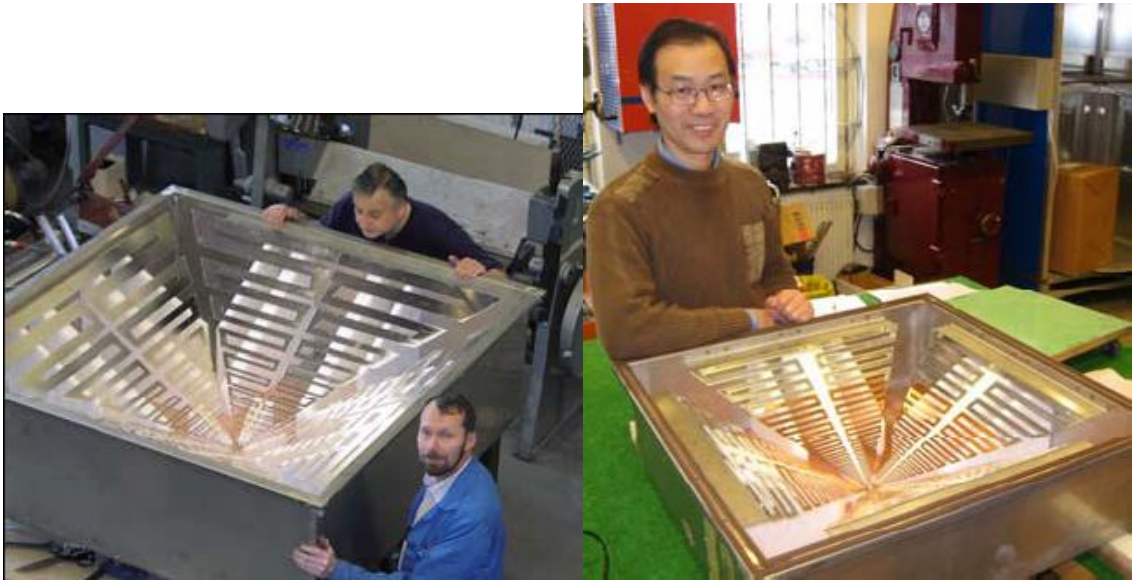


Fig. 1.4. Models of “eleven” antennas, developed for usage in radio telescopes Green Bank (left) and RATAN (right).

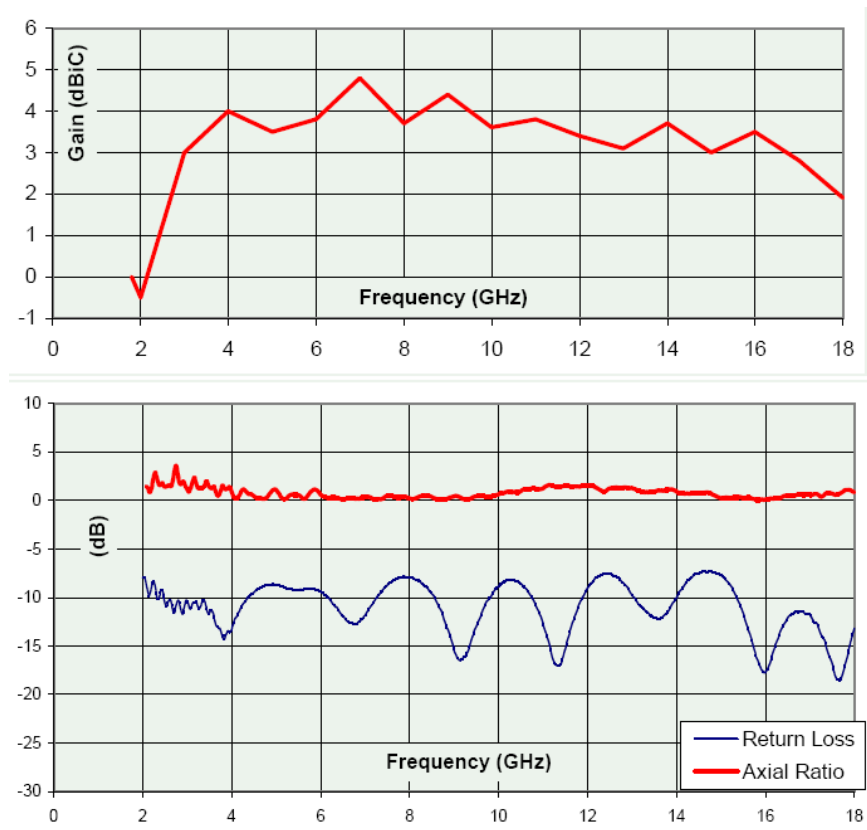


Fig. 1.5. Characteristics of the spiral antenna being used.

Because the gain of the spiral antenna, that is being used, is small, the decision was made for modelling the irradiator in the form of quad ridged horn and “eleven” antenna. Based on results one of them was chosen for future work.

2. QUAD RIDGED HORN ANTENNA

2.1. Modelling the horn

Design of the UWB quad ridged horn antenna of double polarization is shown in the figure 2.1 below. Total length of antenna is 86.5 mm with aperture dimensions of $59 \times 59 \text{ mm}^2$. Antenna can be divided into two parts: circular waveguide of constant diameter, and conical horn, with ridges in both parts. At the lower end of antenna is located a shorting plate.

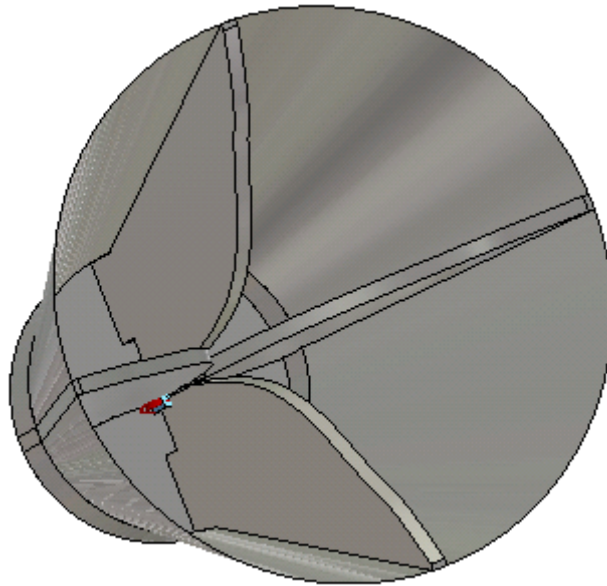


Fig. 2.1. Model of the horn antenna as the irradiator.

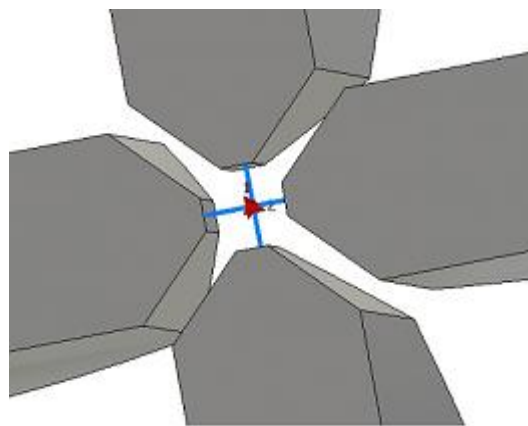


Fig. 2.2. Two ports of the quad ridged waveguide without the coaxial cables.

Quad ridged waveguide consists of four ridges of two orthogonal polarizations. For the single-mode operation widening the frequency range between TE₁₀ and TE_{20L} modes and impedance matching with coaxial cable (50 Ohms) can be achieved by placing the ridges with a short gap between them. At first, two ports of quadruple waveguide without coaxial cables were modeled for one mode (TE₁₀) in 2-16 GHz frequency range, using CST Microwave studio program. Dimensions of ridges at the bottom of antenna and radius of waveguide are shown in the fig. 2.3. They were obtained during optimization of several parameters that define the geometry of lower part of the horn. That is important for the lowest frequency, at which waveguide becomes evanescent. These parameters are:

- 1) horn radius at the throat;
- 2) ridge-to-ridge gap width g ;
- 3) ridge thickness t ;
- 4) ridge tip width w .

Moreover, last three depends on each other. As was checked, lowering the gap width between the ridges $g \rightarrow 0$, cutoff frequency is decreased (up to 4 times). Increasing the ridge's thickness also decreases the cutoff frequency, but not that much. Matching with coaxial cable should also be taken in consideration. That is why dimensions that are shown at the fig. 2.3 were taken.

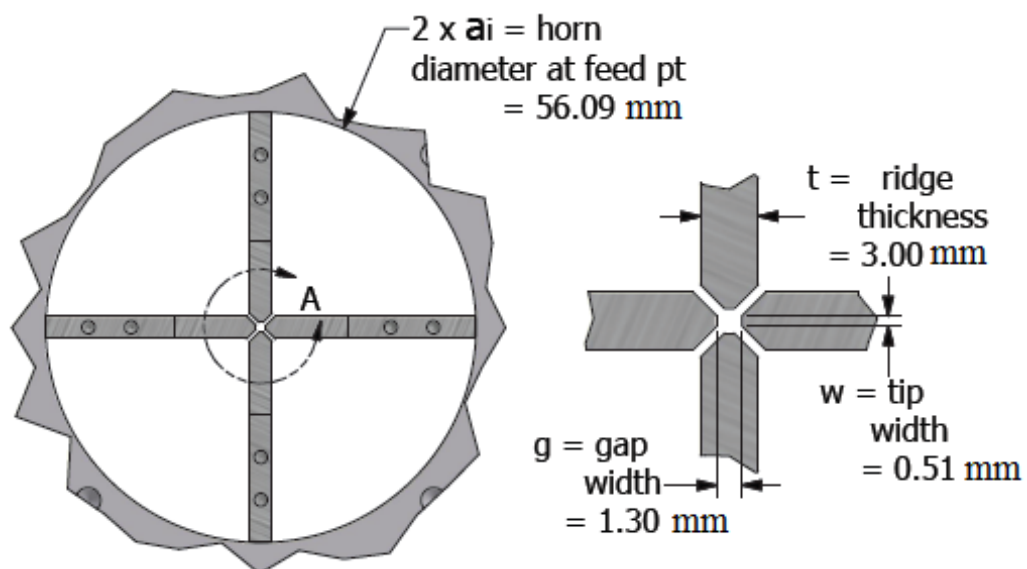


Fig. 2.3. Ridge dimensions at the throat of antenna.

Another consideration for selecting the profiles of the ridges and sidewall is that the gap between the ridges should be sufficiently small in any cross section along the longitudinal axis of the horn to provide the propagation of the dominant mode in the desired frequency range. The cutoff frequency of the dominant mode depends on the gap width, and minor increase of the width of

the gap is possible only with increasing the radius of the outer sidewall of the horn. This, in turn, makes the horn to be able to excite high order modes.

Horn throat radius, ridge-to-ridge gap width and the profiles of ridges are important factors for determining the lowest frequency, at which radiation may take place. The gap width, together with ridges thickness also determines the input impedance of the horn. The smaller the gap, the lower the input impedance and visa versa. Same effect can be achieved by increasing the thickness of ridges.

The next step is creation of the junction between two coaxial cables and quad ridged horn. One coaxial cable is needed for vertical polarization, and the second for horizontal. Options for the cable's connections are important due to the losses related to the backward radiation. For good isolation and low return loss two conditions were revealed:

- 1) The inner conductor of coaxial cable should go through the first ridge and then be connected to the opposite one. Schematically this condition is shown on the fig. 2.4. for the spot, where the coaxial cable is entering into the horizontal ridges of the waveguide.
- 2) Inner conductor and the cable's braid should be connected to ridges very close to its ends.

It is important to use the shorting plate at the end of the waveguide to decrease the losses related to the backside radiation. In the present model simple circle plate was used for this purpose (Fig. 2.5). Distance between the end of the waveguide and the plate is equal to 7.04 mm. For better effect in this gap lossy material could be placed.

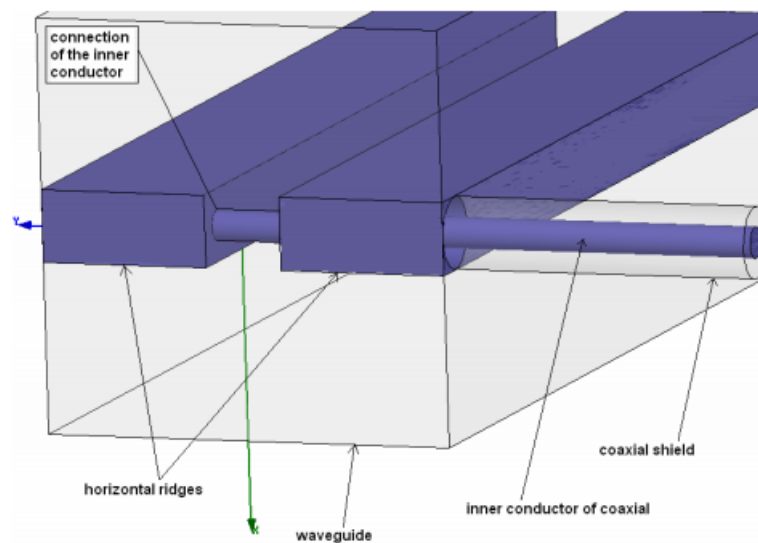


Fig. 2.4. Junction of the coaxial cable with the ridges of the waveguide [5].

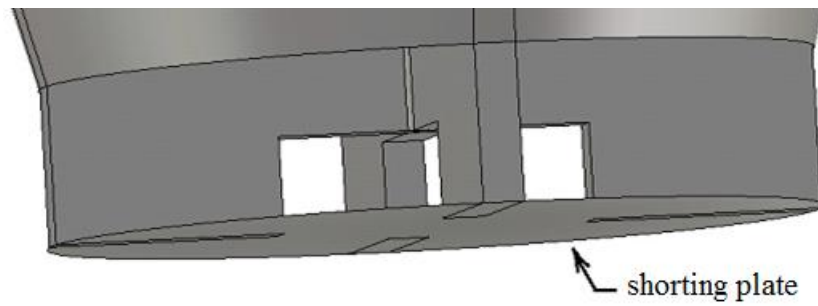


Fig. 2.5. Usage of the shorting plate for decreasing losses for the backward radiation.

The last step of antenna modelling is constriction of four identical ridges. Smooth transition from the waveguide impedance (50 Ohms) to the free space impedance (377 Ohms) should be achieved with the height and width of the ridges. In some similar schemes development of different functions were taken as basis for ridges profile. In this work, exponential function was taken as the bases for their profile:

$$a(z) = \frac{a_0 - a_i}{e^{R \cdot L} - 1} \cdot e^{R \cdot z} + \frac{a_i \cdot e^{R \cdot L} - a_0}{e^{R \cdot L} - 1} \quad (1)$$

In this function a_i and a_0 are radiuses at the feed point and aperture, respectively, L is the length of the horn, R is coefficient, showing the speed of horn's opening. Coefficient R is mainly responsible for the tapering angle β , which has huge influence at the beamwidth of antenna and cutoff frequency. In our case, after some optimization procedures, optimal value of angle $\beta = 60^\circ$ was chosen, which is achieved by the value $R = 0.0338$. The length of the horn $L = 100 \text{ mm}$ and aperture radius $a_0 = 54.5 \text{ mm}$. About 10 points were calculated in Mathcad by equation (1) that later on were imported to the CST Studio and converted to spline that built the profile of the ridges.

Significant part of the time was used to optimize the profile to improve such parameters as beamwidth at -3 dB level, phase center stability and VSWR value. This is because calculation of one model lasts for a half an hour using modern computers. Results of modelling are presented below.

2.2. Results of modelling and optimization

Graphs for the non-optimized horn are shown in the fig. 2.7.

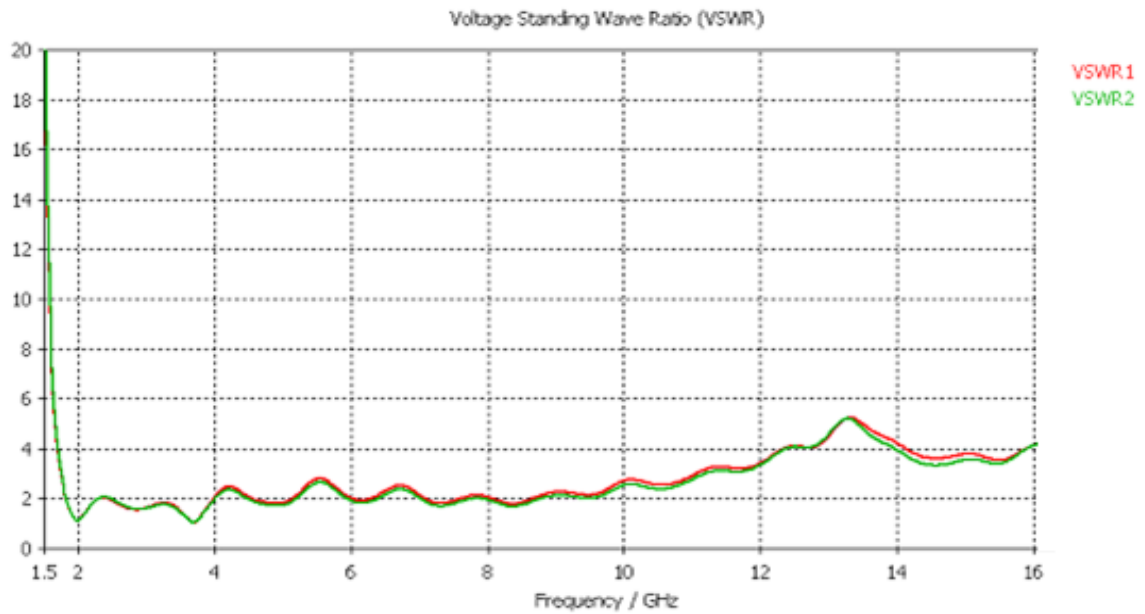


Fig. 2.7. VSWR of the initial horn.

VSWR that is shown in the fig. 2.8. was achieved after optimization of the ridges profiles and scaling of the entire horn.

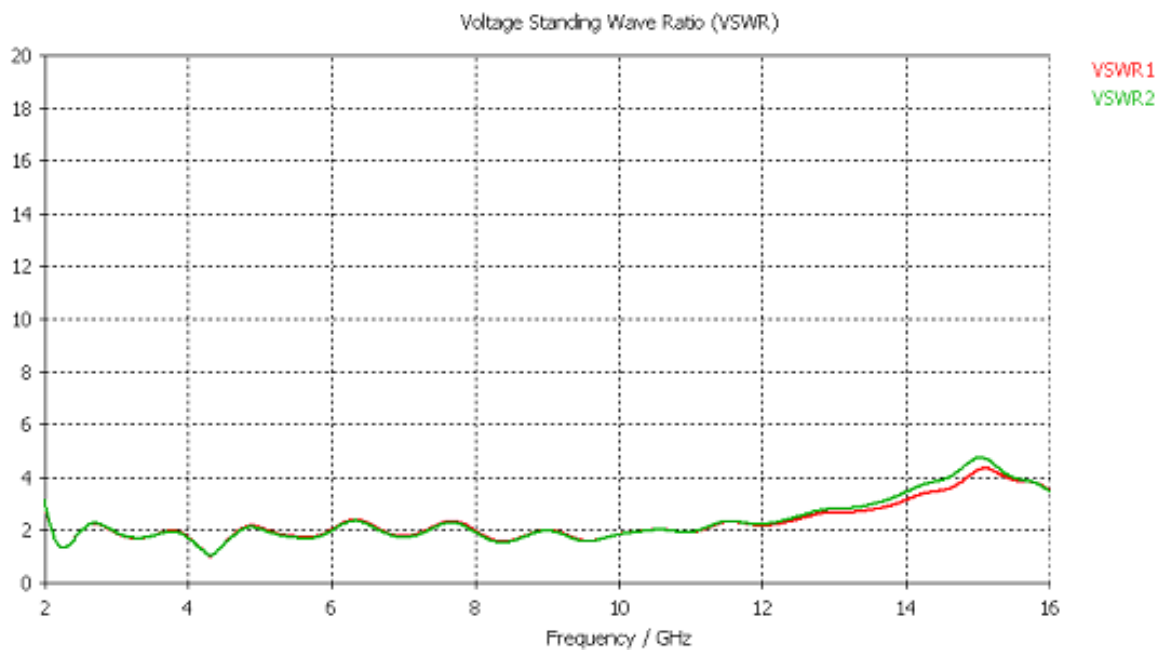


Fig. 2.8. VSWR of the optimized horn.

From 2 to 12 GHz VSWR is less than 2, and only on high frequencies it increases up to 3-4. Ports 1 and 2 have almost no influence on each other. It can be seen on Fig. 2.9.

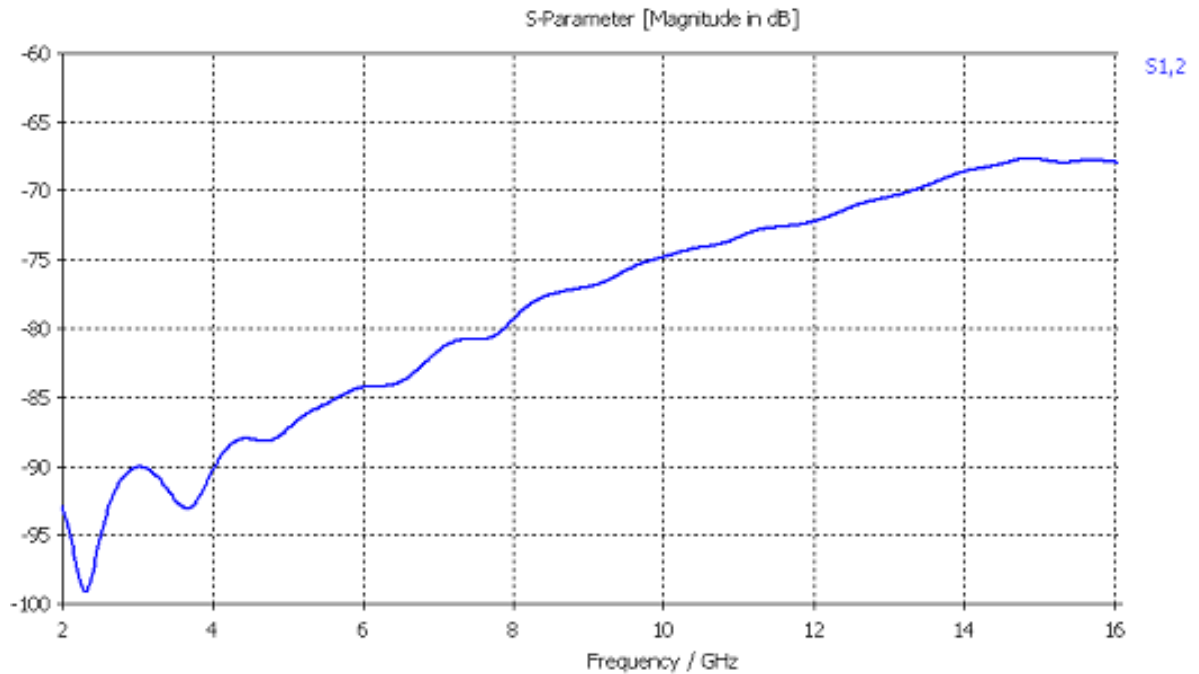


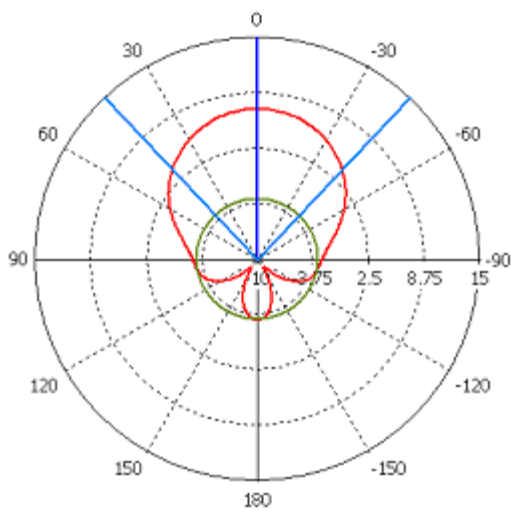
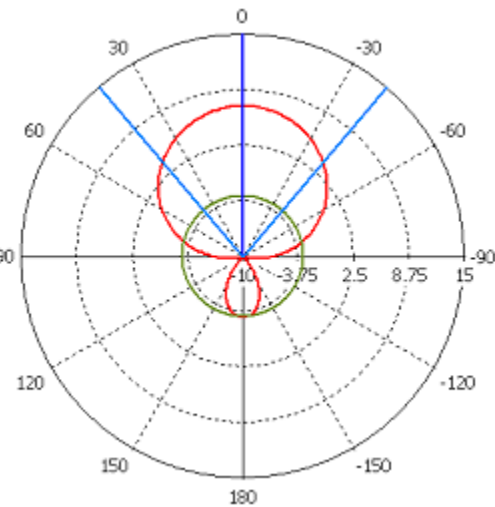
Рис.2.9. Dependence of S12 coefficient from frequency.

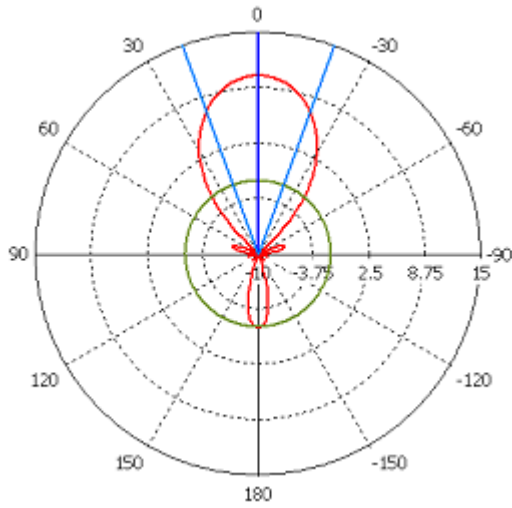
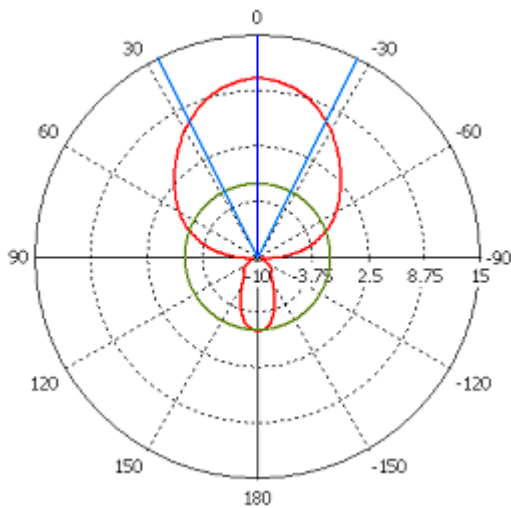
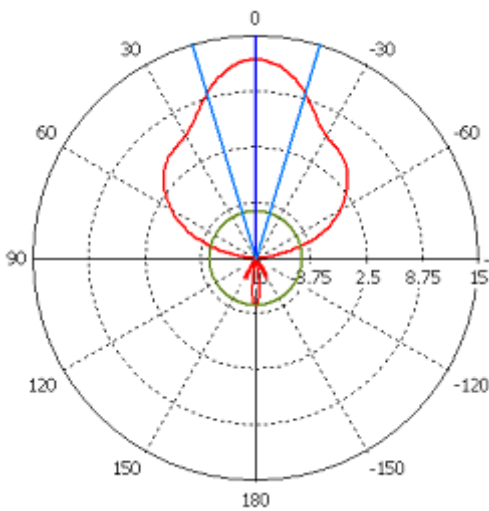
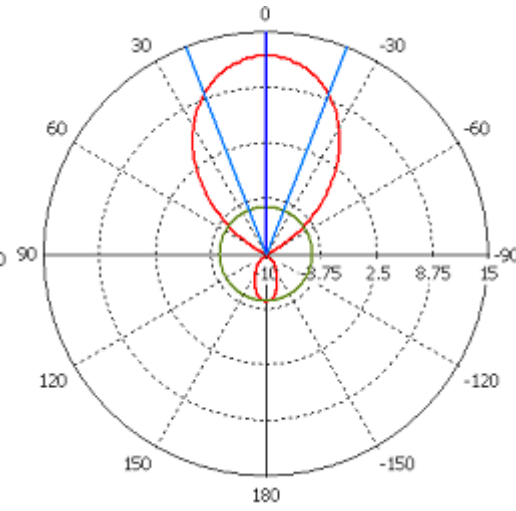
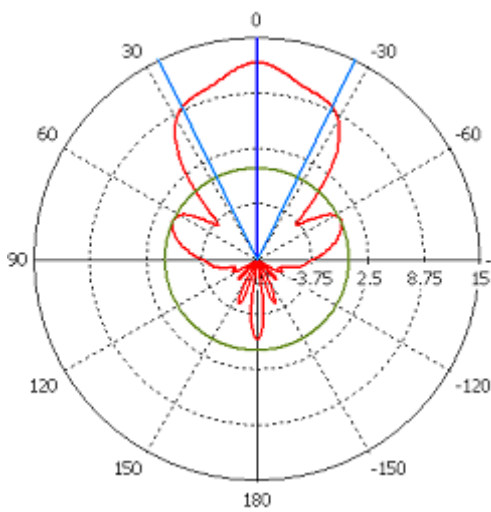
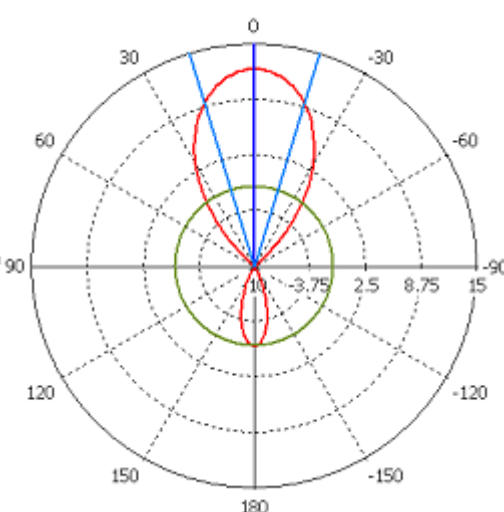
Main characteristics of antenna on different frequencies are shown in table 1 below. Directivity patterns of the horn for frequencies 2-16 GHz are shown on Fig. 2.10 – 2.25. It can be seen that levels of backwards radiation and side lobes are sufficiently small until 12 GHz. From 12 to 16 GHz that effect was not achieved, and high side lobes levels can be seen. Phase center of antenna is also unstable and moving with changing frequency. Also from the modelling the fact that gain is identical for horizontal and vertical polarization was found. Beamwidth is also small from 12 GHz and higher. However, that antenna is good for frequencies 2-12 GHz and could be used for purposes that do not require 9:1 bandwidth.

Table 2.1. Main characteristics of antenna

Frequency (GHz)	Beamwidth at -3 dB (°)	Side lobes level (dB)	Phase center of antenna coordinate (Z axis, mm)	Angle ϕ (°)
2	86,8	-10.1	100	0
2	81,3	-10.0	94	90
4	39,8	-11,8	76.9	0
4	53,5	-11,8	118	90

6	33,2	-17,0	94.6	0
6	42,3	-17,0	55.4	90
8	52,2	-11,7	97.3	0
8	33,9	-13,2	54.4	90
10	42,5	-9,6	80.7	0
10	28,6	-16,2	45.8	90
12	41,3	-19,9	119.4	0
12	18,0	-19,1	51.8	90
14	30,6	-11,6	121.5	0
14	14,4	-11,2	40.8	90
16	13,9	-2,5	39.5	0
16	11,7	-6,6	40.1	90

Fig. 2.10 $f=2$ GHz, $\varphi=0^\circ$ Fig. 2.11. $f=2$ GHz, $\varphi=90^\circ$

Fig. 2.12. $f=4$ GHz, $\phi = 0^\circ$ Fig. 2.13. $f=4$ GHz, $\phi = 90^\circ$ Fig. 2.14 $f=6$ GHz, $\phi=0^\circ$ Fig. 2.15. $f=6$ GHz, $\phi=90^\circ$ Fig. 2.16 $f=8$ GHz, $\phi=0^\circ$ Fig. 2.17. $f=8$ GHz, $\phi=90^\circ$

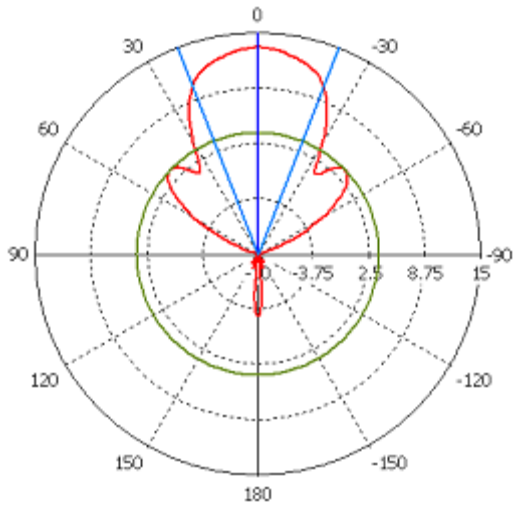


Fig. 2.18 $f=10\text{ GHz}, \varphi=0^{\circ}$

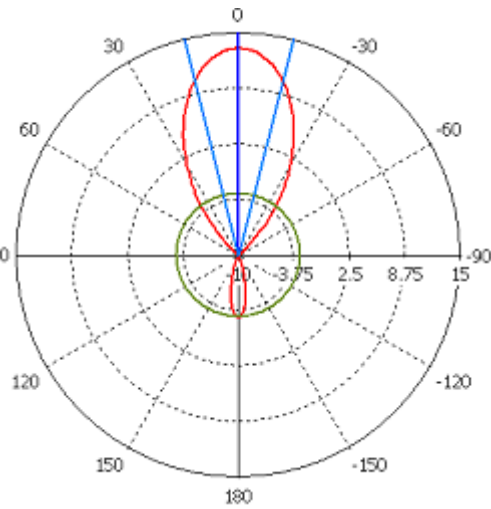


Fig 2.19. $f=10\text{ GHz}, \varphi=90^{\circ}$

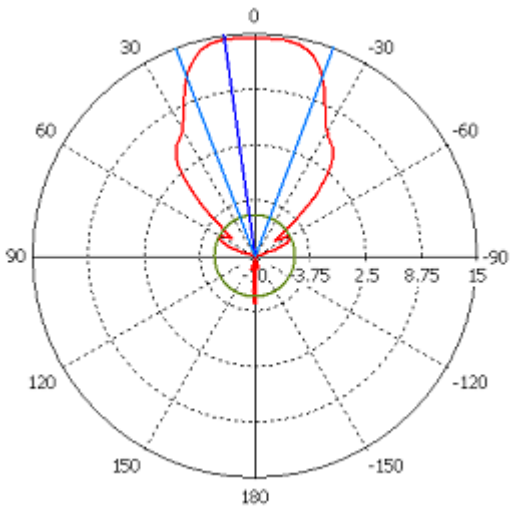


Fig. 2.20 $f=12\text{ GHz}, \varphi=0^{\circ}$

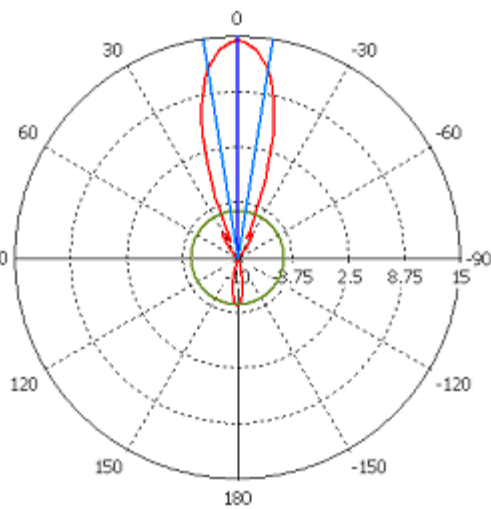


Fig. 2.21. $f=12\text{ GHz}, \varphi=90^{\circ}$

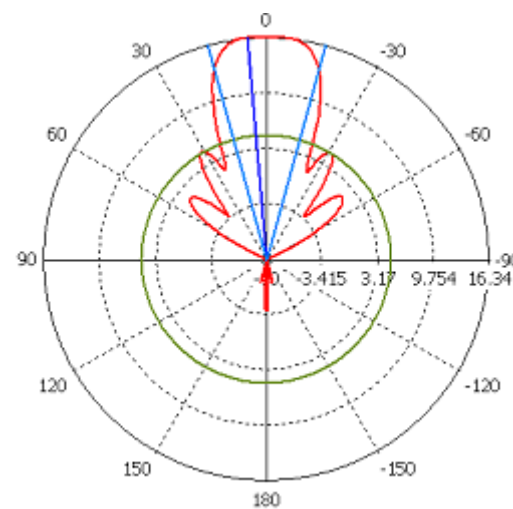


Fig. 2.22 $f=14\text{ GHz}, \varphi=0^{\circ}$

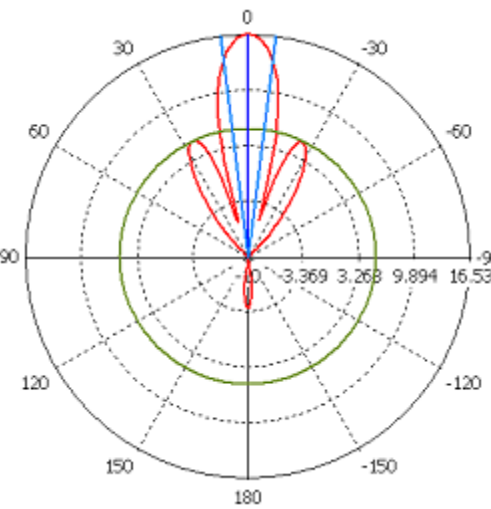


Fig. 2.23. $f=14\text{ GHz}, \varphi=90^{\circ}$

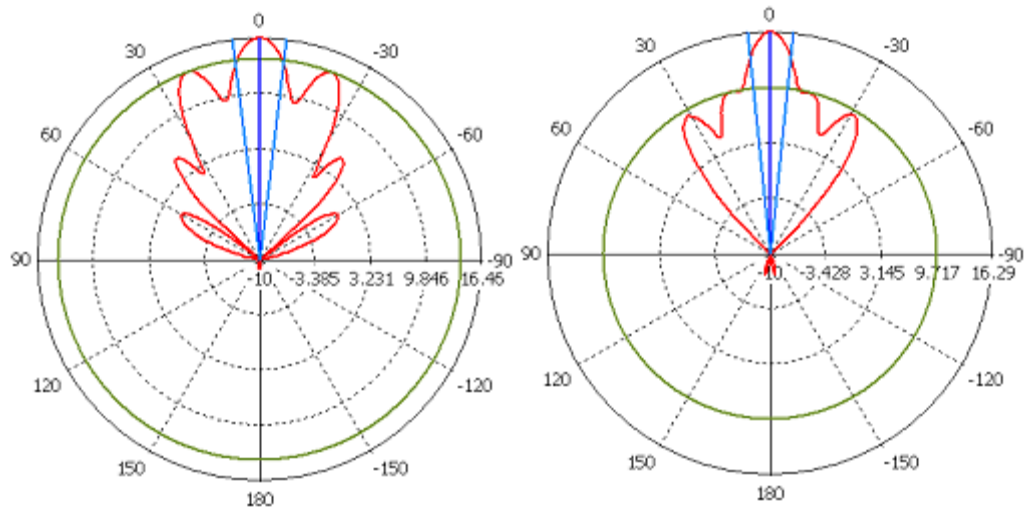


Fig. 2.24 $f=16$ GHz, $\varphi=0^\circ$ Fig. 2.25. $f=16$ GHz, $\varphi=90^\circ$

2.3. Conclusions

At this stage of the work construction of the dual-polarized UWB horn antenna was considered. One of the main advantages of this antenna is the fact that feed point of such antenna is made with minimum soldering. That is very important for matching it with coaxial cable. Results of modeling showed acceptable VSWR (<2.2), gain, beamwidth at -3 dB and phase center stability in 2-12 GHz frequency range. However, from 12 to 16 GHz results are worse, and acceptable parameters were not achieved. Also this model has significant backward radiation at low frequencies and phase center instability in quite wide frequency range. Due to all these factors decision to study another type of antenna had been made, namely “eleven” log-periodic antenna (model is shown on fig. 3.1.). This antenna is harder to be produced, but better characteristics are expected, namely wider beamwidth at high frequencies and phase center stability.

3 “ELEVEN” ANTENNA

3.1. Modelling the irradiator in the form of “eleven” antenna

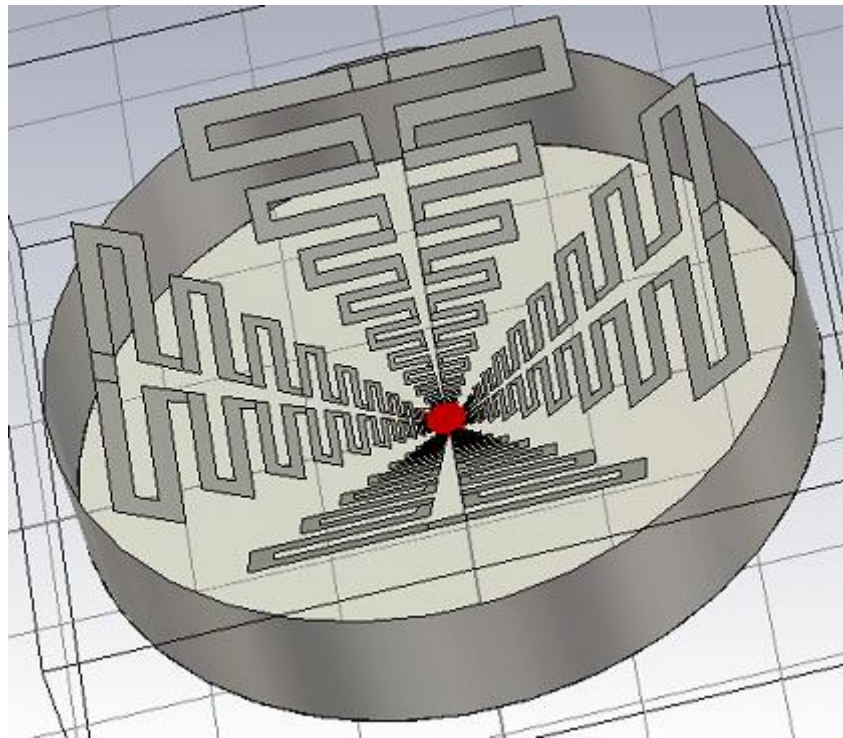


Fig. 3.1. Model of “eleven” antenna at the initial stage of development.

Based on the experience of development "eleven" antennas, work of this type of antennas in a wide frequency range is achieved by building a cascade of logarithmic scaled elements. Petals of antenna were designed on the bases of PCB of 0.25 mm thickness, with the parameters $\varepsilon = 2.2$, $\mu = 1$, which correspond to the parameters of the material RT/duroid 5880 (firm Rogers) [14] on the basis of which is planned the creation of a physical model. Modeling and subsequent optimization was performed in CST Microwave Studio. Copper dipoles in the design were assumed to be infinitely thin. The whole model was specified parametrically, for the convenience of changing its parameters. The scaling factor k was changed during optimization, its final value is shown in Table 3.1. The length of the first dipole of the antenna was given as sine and cosine of angles and parameters r_0 , d_1 , d_2 , x_1 , x_2 (see Fig. 3.3). In the future, when changing the angles and these parameters, the length, width, aperture and tilt angle of the ends of the dipoles of the entire antenna were also changed to obtain acceptable parameters of matching, beamwidth and the form of directivity pattern. The diameter of the hole in the two-mirror antenna system, where this antenna is supposed to be placed, that is equal to 110 mm, was the constraint for the dimensions in the design of the antenna. Due to this, for the reduction of the radiation to the lower hemisphere and undesired angles areas, bottom plate of such diameter and side plate with

the height of 22 mm, along its perimeter, were modelled. Initially structure was considered in the form of straight dipoles of the same width, as it was shown in Fig. 3.1., but later form dipoles had been modified to improve the performance of the antenna. The final type of feed is presented in Fig. 3.2 below. Basic dimensions of the final antenna shown in Fig. 3.3. and Table 3.1.

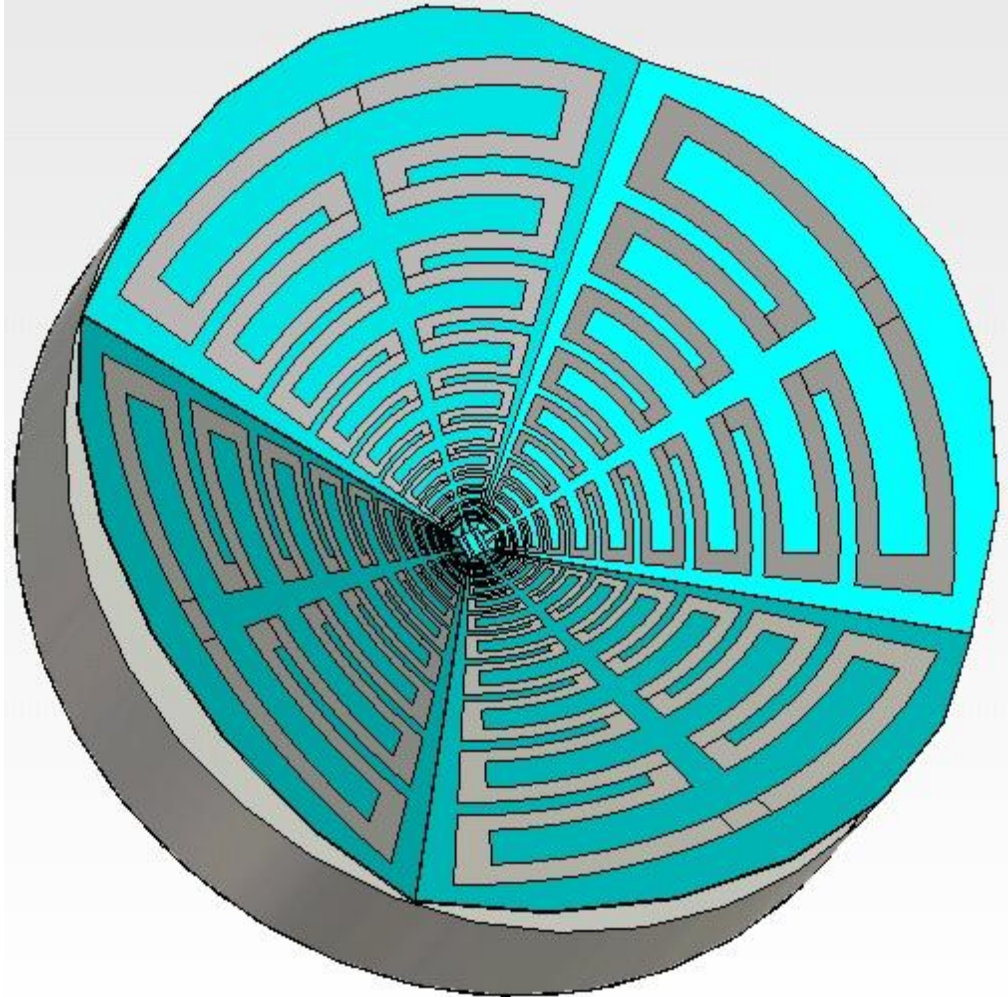


Fig. 3.2. Final model of the “eleven” antenna.

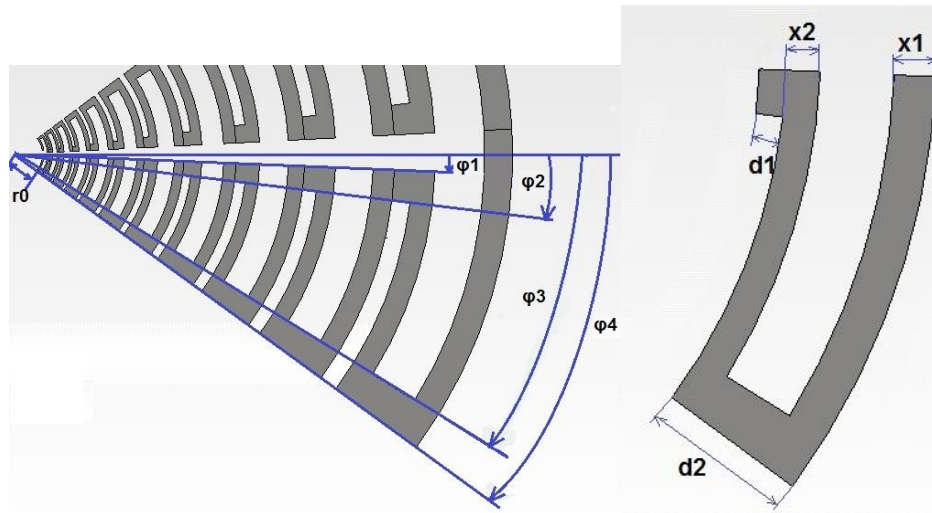


Fig. 3.3. Angles, that were used for creating the antenna (left) and the dimensions of the first dipoles (right).

Table 3.1. Geometrical parameters of antenna.

Parameter	Value	Parameter	Value
$\varphi 1$	$3,7^0$	$r0$	2.22mm
$\varphi 2$	$6,2^0$	$d1$	0.11mm
$\varphi 3$	29^0	$d2$	0.73mm
$\varphi 4$	$34,5^0$	$x1$	0.22mm
k	1.111	$x2$	0.25mm
ang	29^0	N	8

First width of vibrators $x1$ and $x2$ was made equal, but better characteristics were achieved by varying them. k is the scale coefficient of all dipoles, starting with first one, ang is the petal's tilt angle, relatively the horizontal plane and N is number of dipoles.

Circular polarization in such antenna is achieved by feeding the adjacent petals of antenna with phase of 90^0 . Feed point of such antenna is assumed as four coaxial cables, central conductors of which are soldered to the parallel (for each polarization) strips that bring power to the log-periodic system of dipoles, and its shields to the body of antenna. Strips for different polarizations are located under each other, divided by the PCB layer. When modelled in CST Microwave Studio, feeding of the antenna was made by discrete ports, located at the end of the coaxial cables parts. Top view at the feed unit of this antenna is presented in the Fig. 3.4.

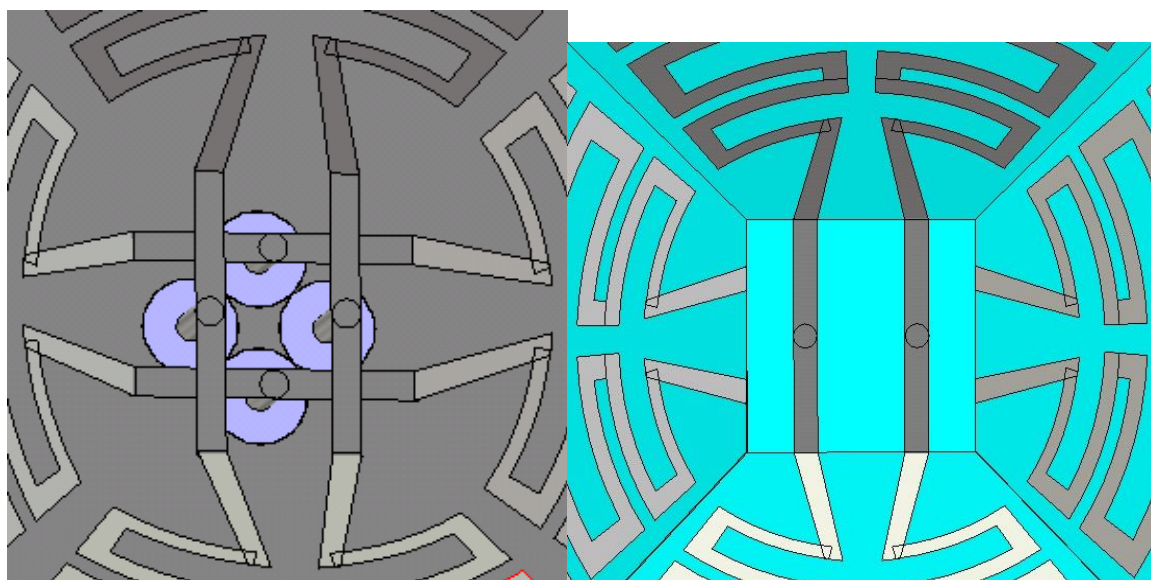


Рис. 3.4. Modelling of the feed unit of the “eleven” antenna in CST Studio.

Scheme of similar feeding of antenna which had been realized in practice is showed in [8]. In it two strips, that connect two opposite petals of antenna, are fed by two cables with phase shift of 180° . For the phase shift antiphase coupler is used with characteristics that are described in [12]. In our case there are two polarizations, so that in addition to two of that couplers, quadrature coupler must be used (with 90° phase shift). Photos of such couplers made by Krytar firm are presented in fig. 3.5 below.



Fig. 3.5. Antiphase coupler (left), quadrature coupler (right).

Proposed realization of feed unit is presented in fig. 3.6 below. That method also allows to match the input impedance of the antenna with impedance of the cable (50 Ohms).

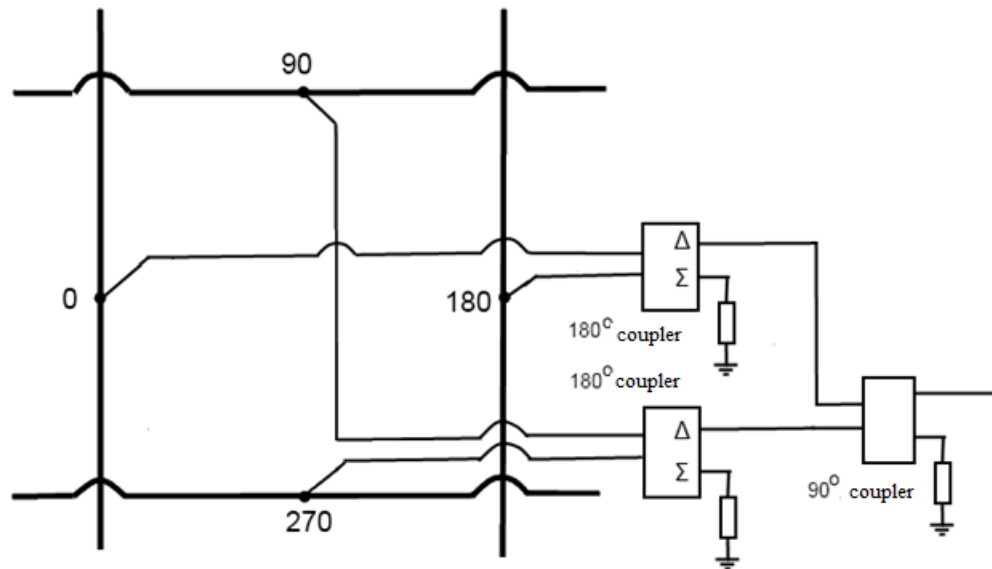


Fig. 3.6. Proposed realization of the feed unit of “eleven” antenna.

3.2. Results of modelling and optimization

Considerable time of investigation the "eleven" antenna was spent on the optimization of its parameters in order to obtain acceptable values of matching and beamwidth at all frequency range. As selection of different parameters showed, the more elements has the antenna, the worse is its matching, but the directivity pattern is wider. Also it depends on the shape of dipoles and their geometrical dimensions and the design of the feed unit. Due to all this, the goal was to find some optimal values, when both matching and directivity pattern would be good. Fig. 3.7 (a) represents the graph of return loss (coefficient S_{11}) of the first model, and Fig. 3.7 (b) an optimized antenna for one polarization, with simultaneous excitation of two ports. It can be seen that as a result of selection right set of parameters, matching was significantly improved across the entire frequency range.

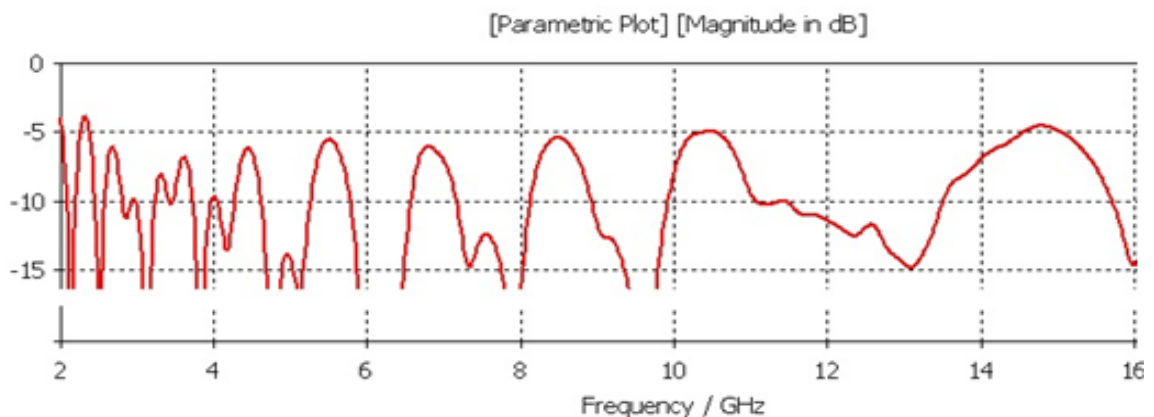


Fig. 3.7(a) Return loss (S_{11} parameter) of the non-optimized antenna

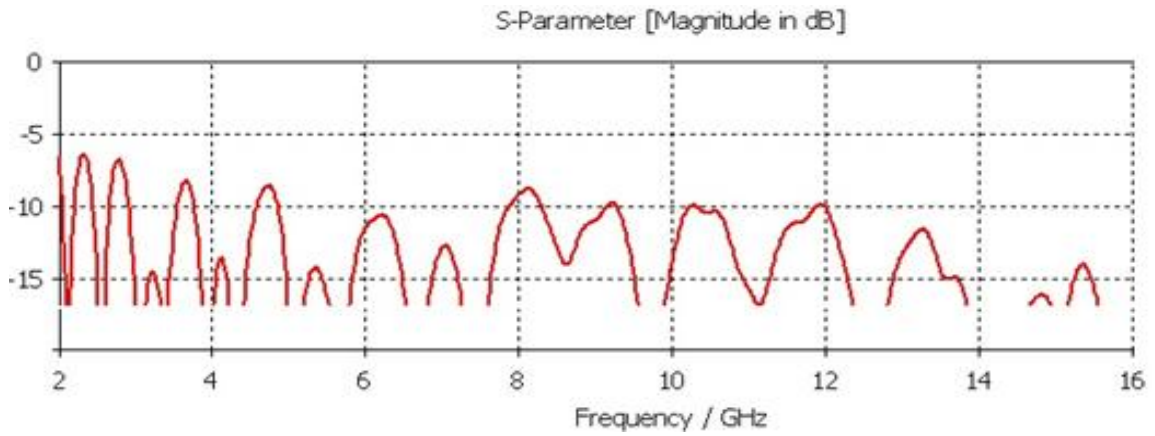


Fig. 3.7(b) Return loss (S_{11} parameter) of the optimized antenna.

Calculation of the parameters of the optimized antenna was made with the alternate feeding of all 4 ports, and later the results were combined with the required phase shifts.

VSWR was obtained by measuring the S_{11} and S_{12} parameters with their phases, and later by subtracting S_{12} from S_{11} in the complex form. That operation was made in the MathCAD with the parameters that were measured in CST Studio. Due to the fact that the 2nd port was directed in the opposite direction in the model, subtracting was changed to addition (3.1).

$$A_{i,1} := A1_{i,1} \cdot e^{i \cdot A3_{i,1} \cdot \text{deg}} + A2_{i,1} \cdot e^{i \cdot A4_{i,1} \cdot \text{deg}} \quad (3.1)$$

Here, A1 is the array of S_{11} amplitude values, A2 is the array of S_{12} amplitude values, A3 is the array of S_{11} phase's values, and A4 is the array of S_{12} phase's values.

Usage of couplers adds phase and amplitude imbalance, so that matching degradation with their usage should be also taken into account. Datasheet of the couplers reveals parameters of phase ($\pm 12^\circ$) and amplitude (± 0.6 dB) deviation. Using them, function that takes into account possible maximum deviation of phase and amplitude was created in MathCAD during work (3.2). Graphs of the reflection coefficient were built using it for all frequency range for both port's pairs, compared with the absence of the imbalance (fig. 3.8-3.9). It should be noted that the formula takes into account both phase and amplitude imbalance, that rarely occur at same frequencies.

$$C_{i,1} := \max \left(\left| A1_{i,1} \cdot e^{i \cdot A3_{i,1} \cdot \text{deg} + i \cdot f} + A2_{i,1} \cdot e^{i \cdot A4_{i,1} \cdot \text{deg}} \cdot 10^{\frac{d}{20}} \right| \right),$$

$$\begin{aligned}
& \left| A_{1i,1} \cdot e^{1i \cdot A_{3i,1} \cdot \text{deg}} + A_{2i,1} \cdot e^{1i \cdot A_{4i,1} \cdot \text{deg} + 1i \cdot f \cdot \frac{d}{10^{20}}} \right|, \\
& \left| A_{1i,1} \cdot e^{1i \cdot A_{3i,1} \cdot \text{deg} + 1i \cdot f} + A_{2i,1} \cdot e^{1i \cdot A_{4i,1} \cdot \text{deg}} \cdot 10^{\frac{-d}{20}} \right|, \\
& \left. \left| A_{1i,1} \cdot e^{1i \cdot A_{3i,1} \cdot \text{deg}} + A_{2i,1} \cdot e^{1i \cdot A_{4i,1} \cdot \text{deg} + 1i \cdot f \cdot \frac{-d}{20}} \right| \right) ,
\end{aligned} \tag{3.2}$$

Where $f = 12 \text{ deg}$, $d = 0.6$.

This equation

The dotted line displays graphs with the imbalance of couplers, solid line displays them without it. It can be seen that imbalance addition influence mainly high frequencies $> 10 \text{ GHz}$. At low frequencies its effect is negligible. Also it could be seen that values of the return loss for different polarizations (different port pairs and petals of antenna) are different. This is related to the fact that all 4 petals of antenna are assumed to be the same, but due to the construction they are located on the different height above the screen (2nd pair of petals is located 0.25 mm higher). Due to that it is almost impossible to achieve equal parameters for both polarizations.

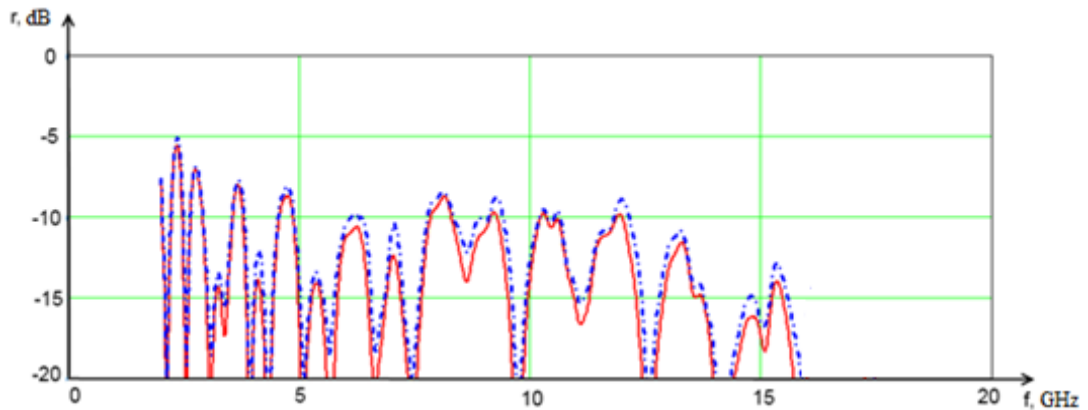


Fig.3.8. Return loss of “eleven” antenna of the 1st pair of ports.

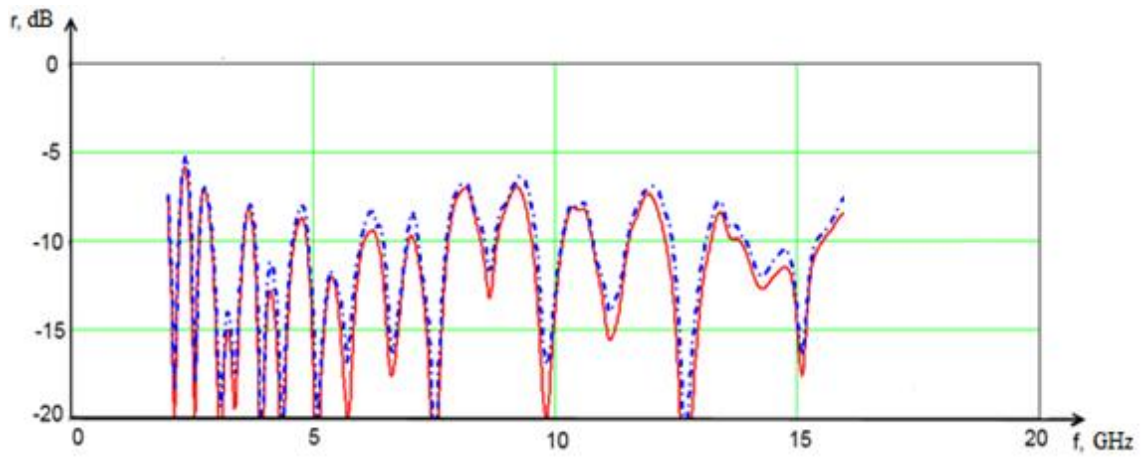


Fig. 3.9. Return loss of “eleven” antenna of the 2nd pair of ports.

From the values of return loss from equation (3.2) (fig. 3.8, 3.9), VSWR could easily be found using (3.3)

$$\text{VSWR} = \frac{1 + r}{1 - r} \quad (3.3)$$

VSWR graphs for both ports are presented in the fig. 3.9 – 3.10.

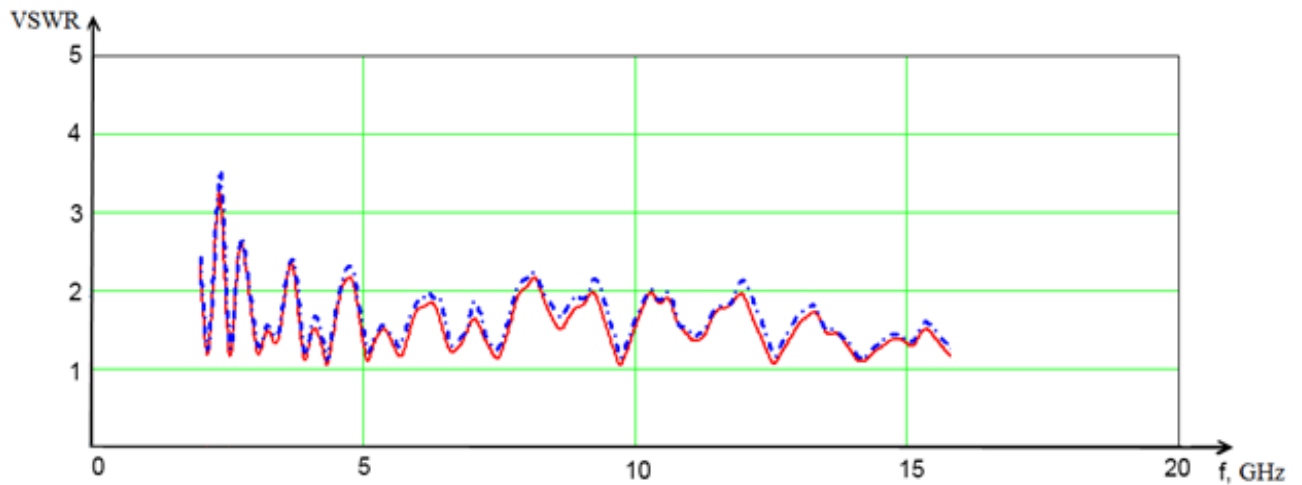


Fig. 3.9. VSWR of the 1st pair of ports.

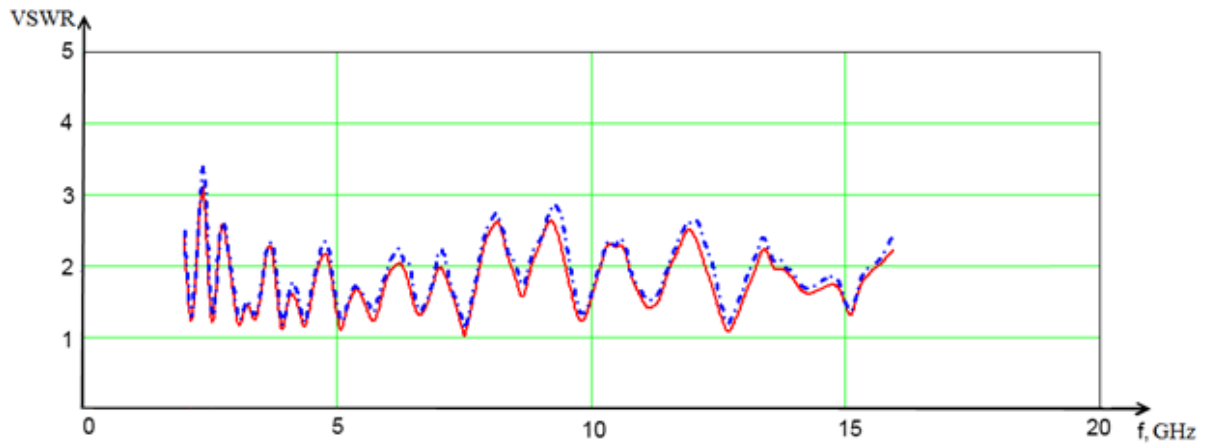


Fig. 3.10. VSWR of the 2nd pair of ports.

Directivity patterns of the antenna for frequencies 2-16 GHz for the values of $\varphi = 0^\circ$ and 45° are presented in the figs. 3.11 – 3.18. Dash dotted line shows directivity patterns for cross polarization.

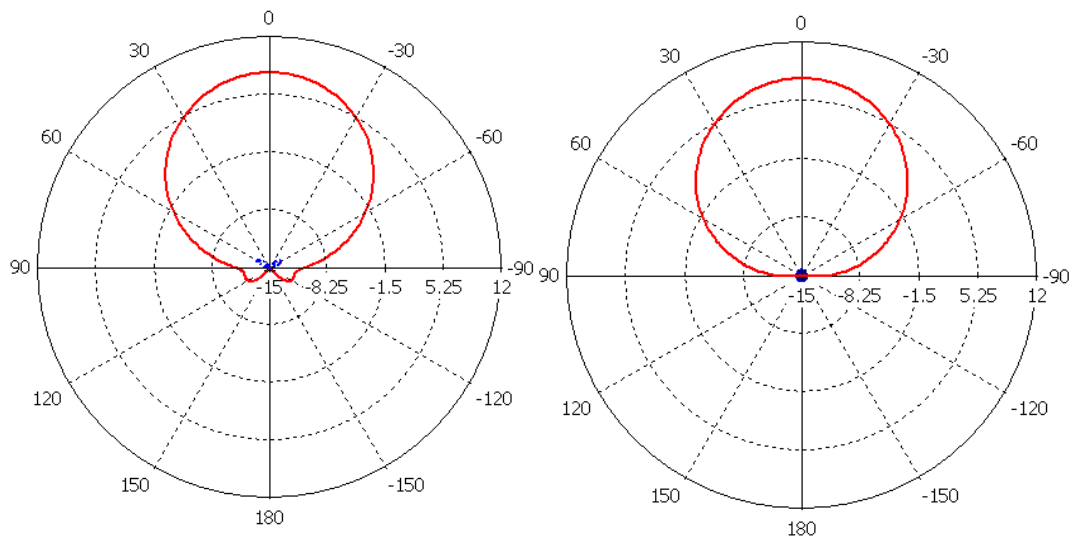
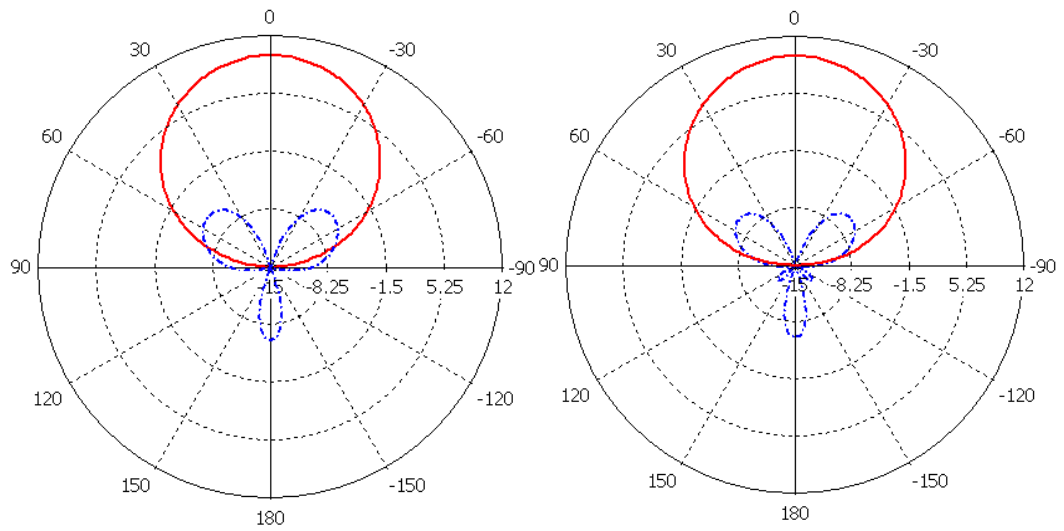
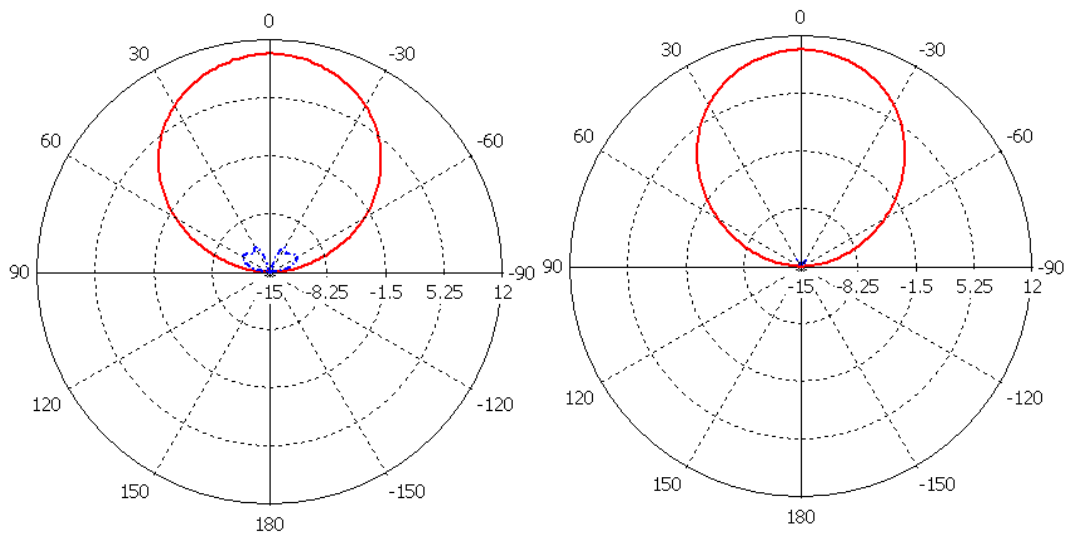
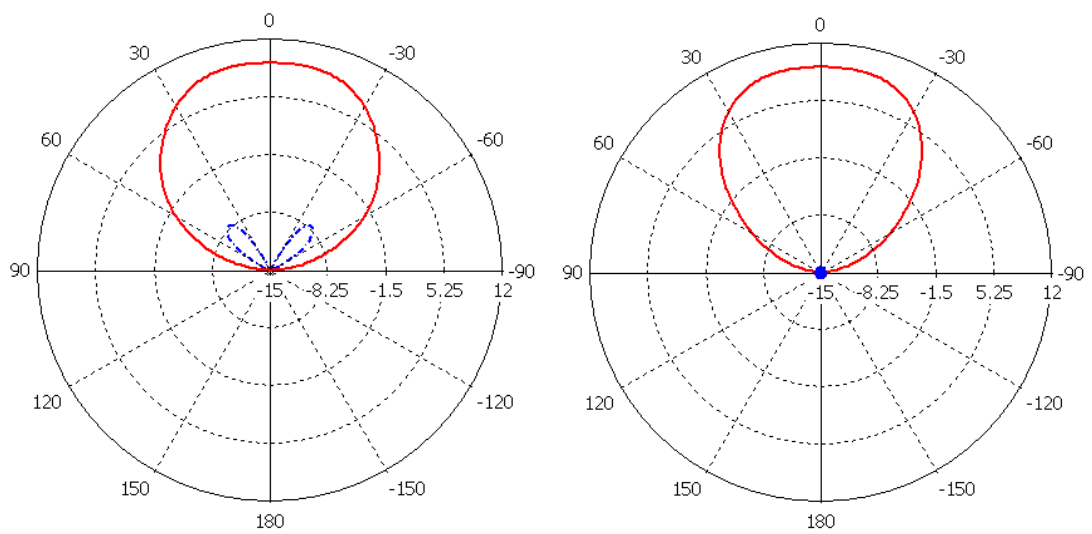
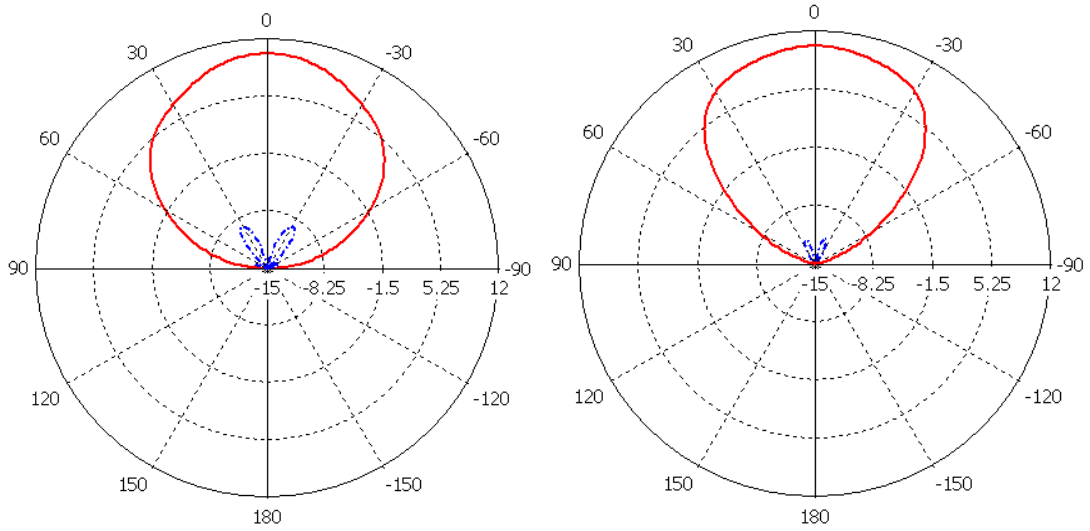
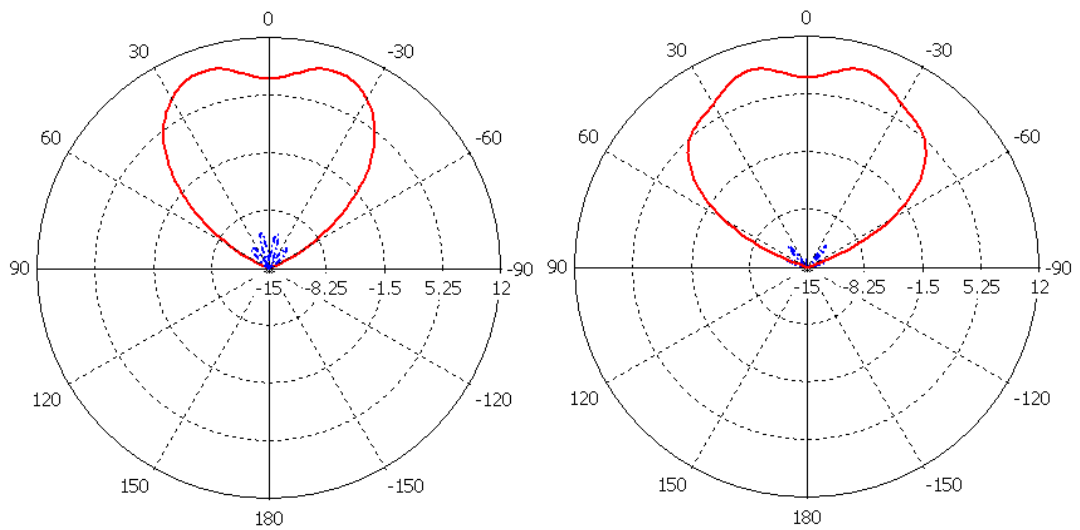
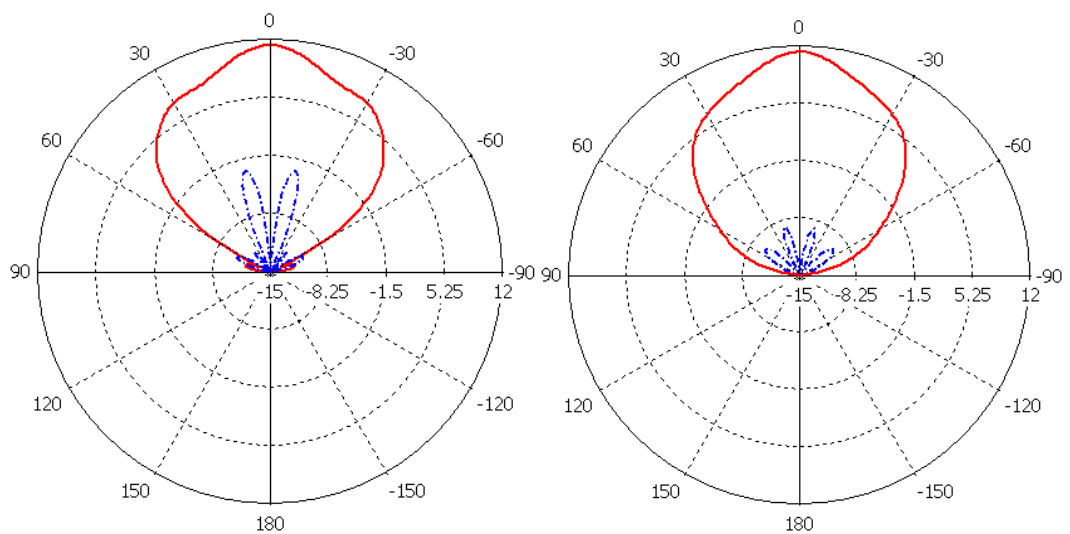


Fig. 3.11. $f = 2 \text{ GHz}$, $\varphi = 0^\circ$

$f = 2 \text{ GHz}$, $\varphi = 45^\circ$

Fig. 3.12. $f = 4 \text{ GHz}$, $\varphi = 0^\circ$ $f = 4 \text{ GHz}$, $\varphi = 45^\circ$ Fig. 3.13. $f = 6 \text{ GHz}$, $\varphi = 0^\circ$ $f = 6 \text{ GHz}$, $\varphi = 45^\circ$ Fig. 3.14. $f = 8 \text{ GHz}$, $\varphi = 0^\circ$ $f = 8 \text{ GHz}$, $\varphi = 45^\circ$

Fig. 3.15. $f = 10 \text{ GHz}$, $\varphi = 0^\circ$ $f = 10 \text{ GHz}$, $\varphi = 45^\circ$ Fig. 3.16. $f = 12 \text{ GHz}$, $\varphi = 0^\circ$ $f = 12 \text{ GHz}$, $\varphi = 45^\circ$ Fig. 3.17. $f = 14 \text{ GHz}$, $\varphi = 0^\circ$ $f = 14 \text{ GHz}$, $\varphi = 45^\circ$

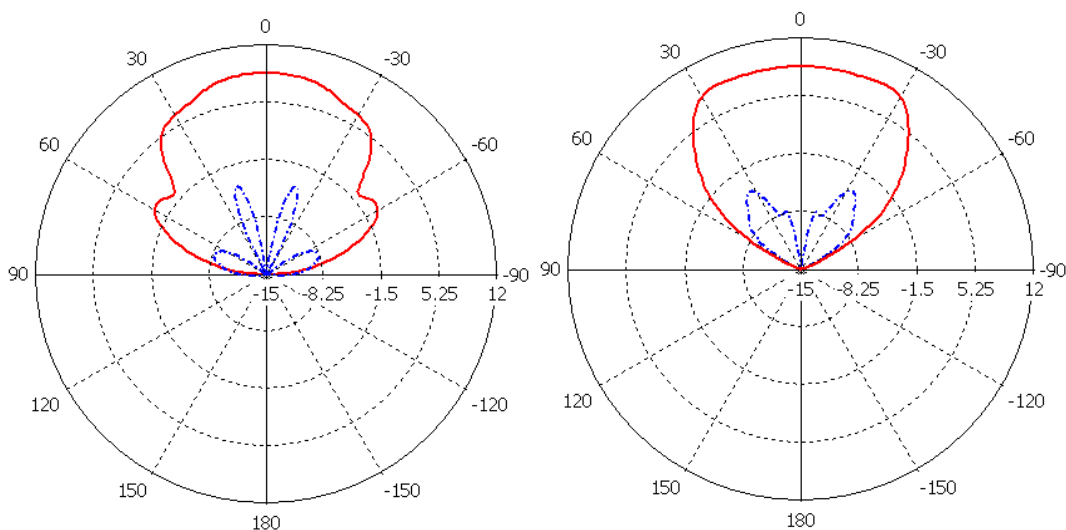


Fig. 3.18. $f = 16 \text{ GHz}$, $\varphi = 0^\circ$ $f = 16 \text{ GHz}$, $\varphi = 45^\circ$

Dependence of gain of antenna from frequency is presented on the fig. 3.20. It can be seen that gain of antenna is $> 9.5 \text{ dB}$ in all frequency range.

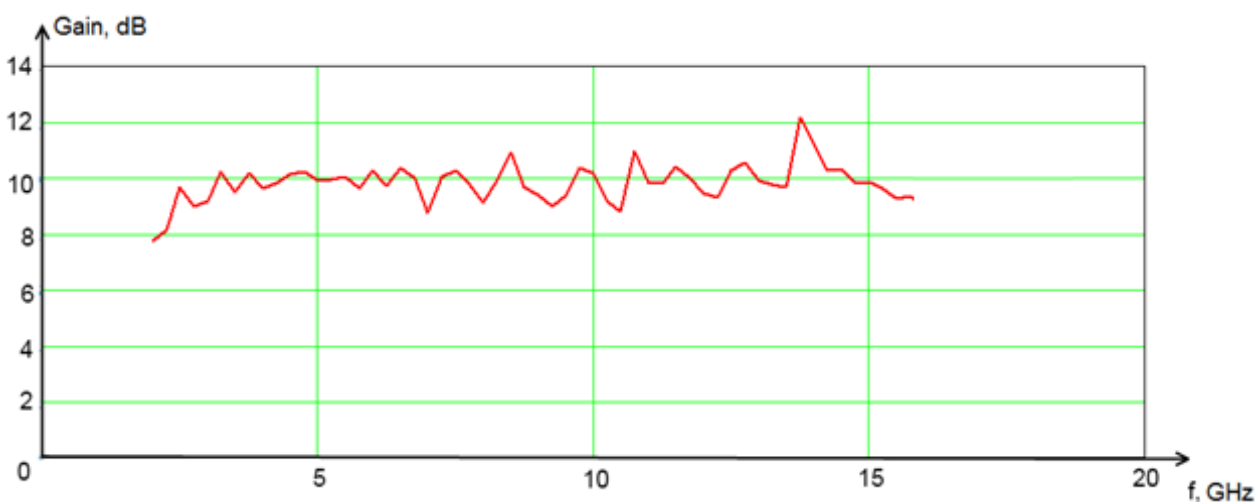


Fig. 3.20. Gain of “eleven” antenna.

Deviation of phase center with frequency (normalized to the wavelength) is presented in fig. 3.21. For almost entire frequency band deviation of phase center is less than 0.25λ . For low frequencies (2-4 GHz), values are slightly over that range and reach 0.4λ . Although it is not good, we were interested in the directivity patterns of the two-mirror system, and the beamwidth of the “eleven” antenna on that frequencies allows to obtain acceptable directivity patterns for the two-mirror system, even with such shift of phase center.

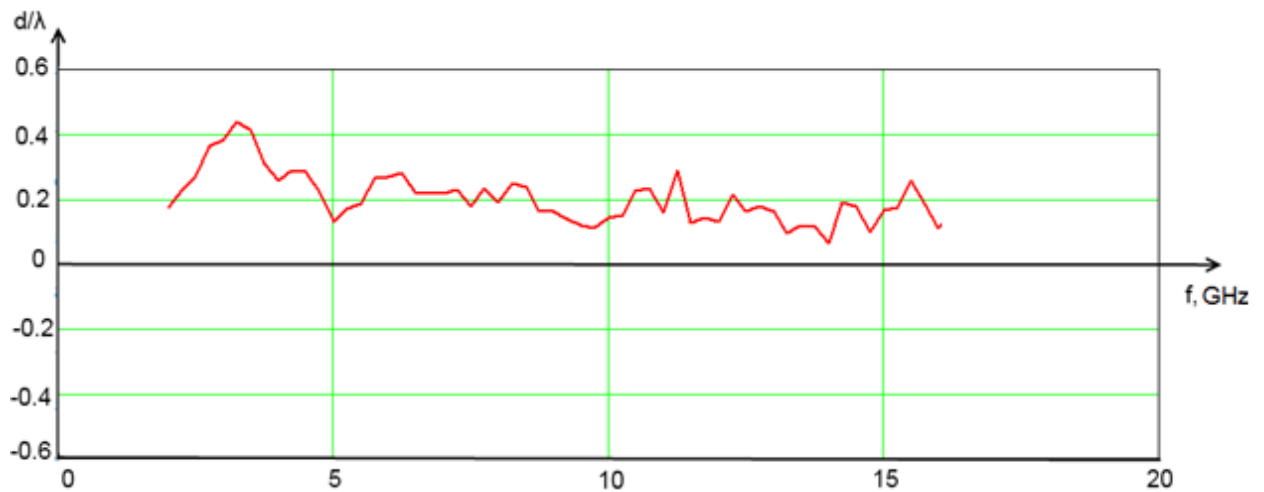


Fig. 3.21. Phase center deviation of “eleven” antenna.

There is also a requirement for the ellipticity at maximum point of the irradiator, it should be less than 3dB. Fig. 3.22 represents the ellipticity coefficient of the “eleven” antenna in all frequency range. It can be seen that its maximum value reaches only 2 dB at high frequencies. For low and average frequencies (< 8 GHz) polarization of the directivity pattern is almost circular. Therefore, the developed “eleven” antenna satisfies all the requirements and can be used as the irradiator for the UWB two-mirror antenna system.

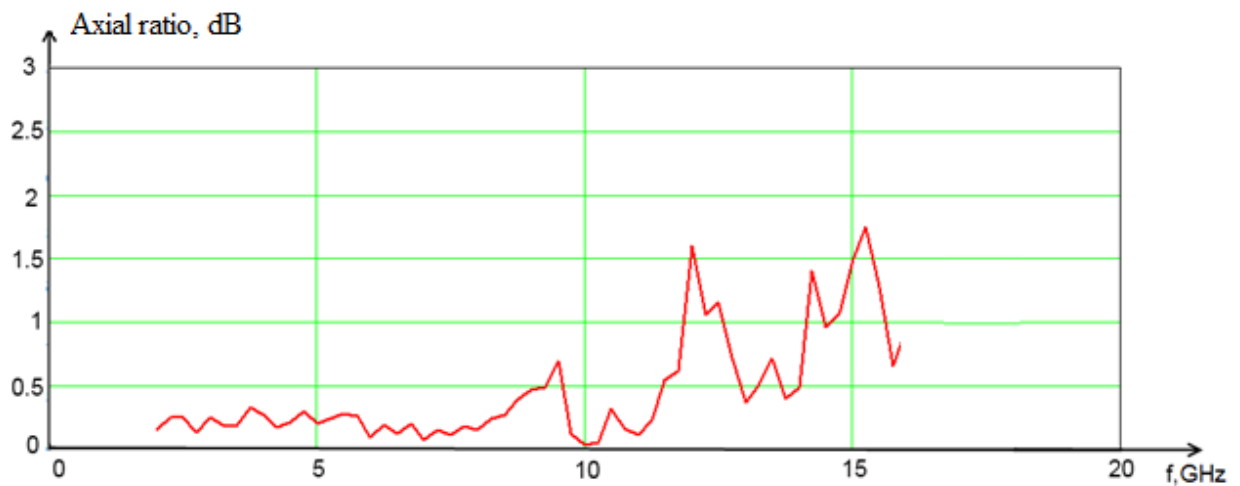


Fig. 3.22. Axial ratio of the “eleven” antenna.

4. TWO-MIRROR ANTENNA SYSTEM

Next step in the development of the feed is to include it into the two-mirror antenna system. Irradiator is supposed to be located in the focus of the upper parabolic mirror (see fig. 4.1). But due to the fact that during development of the “eleven” antenna was obtained that the phase center is shifted upwards ($\sim 0.2 \lambda$ as average), the decision was made to move the irradiator down from the focus point on that distance. Model of two-mirror system consists of parabolic and conical mirrors. Form of conical mirror is given by complex function. That takes into consideration the beamwidth, allows to get required angles of radiation and direction of the main maximum of the two-mirror system. Presence of the additional plates of radio absorbing material allows to minimize the radiation in the direction of undesired angles. Due to the fact that it is impossible to calculate the model of irradiator in the construction of entire system, instead of irradiator farfield sources were used. Phase center shift was taken into consideration by shifting the source from the focus of two-mirror antenna model to the distance, equal to the phase center shift of the irradiator. As result, directivity patterns were obtained for the main (circular) polarization. One of them for frequency $f = 14$ GHz is presented in fig. 4.2. Axial ratio for final two-mirror system was also obtained, and shown in fig. 4.3.

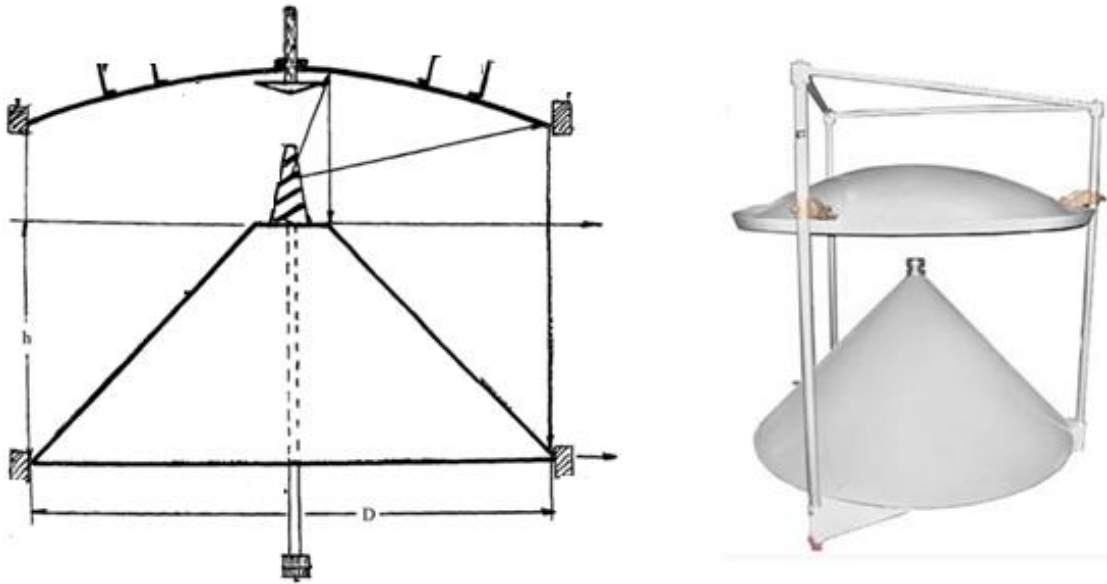


Fig. 4.1 Two-mirror antenna system.

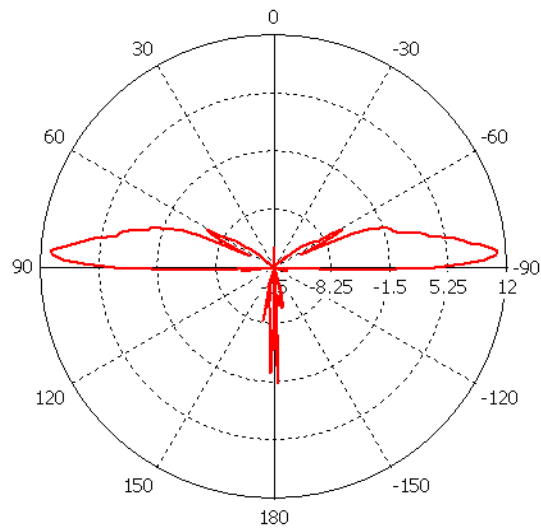


Fig. 4.2. $f = 14$ GHz.

Axial ratio for the two-mirror system is presented in fig. 4.3.

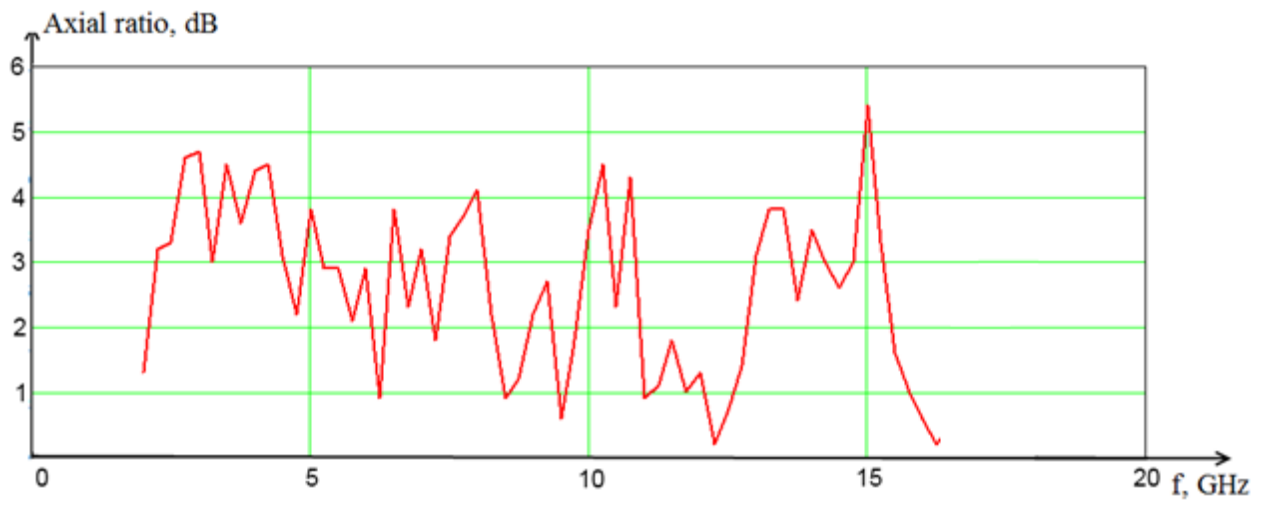


Fig. 4.3. Axial ratio of two-mirror antenna system.

CONCLUSIONS

As the result of this work quad ridged horn was studied as a possible option for the irradiator in the two-mirror antenna system. It was obtained that in the required dimensions this antenna cannot cover required frequency band with desired characteristics, but is able to cover 2-14 GHz band. "Eleven" antenna irradiator was developed for UWB omnidirectional antenna system, made on the two-mirror scheme basis, using CST Microwave Studio software. For "eleven" antenna directivity patterns were obtained from 2 to 16 GHz. The results met requirements for gain that is > 9.5 dB in entire frequency range, phase center stability (significant shift at low frequencies do not influence directivity pattern of the final two-mirror antenna system), polarization and axial ratio at maximum (for the axial ratio of the final directivity patterns, mainly difference in the directivity patterns of horizontal and vertical polarization of the initial source has influence, that were obtained during the "eleven" antenna modelling). Radiation to the lower hemisphere is almost absent. Directivity patterns for the two-mirror system were obtained, using the directivity patterns of the "eleven" antennas.

Main drawbacks of the developed irradiator are the following: phase center shift at low frequencies (2-4 GHz), high VSWR at low frequencies (2-3 GHz), losses in the feed unit and phase deviation due to usage of couplers.

Perspectives of future work are changing the form of cone of the two-mirror system, using the specifics of "eleven" antenna characteristics, creating the physical model and obtaining practical results.

Bibliography

- 1) R. Kjun, Microwave antennas – 1967, 520
- 2) Quad-Ridged Flared Horn, Thesis by Ahmed Halid Akgiray, California Institute of Technology, 2013
- 3) Kerr, J. L., “Short axial length broad-band horns,” IEEE Trans. Antennas Propag., Vol. AP-21, No. 5, 710–714, Sep. 1973.
- 4) Elliptically shaped Quad-Ridged Horn Antennas as Feed for a Reflector, O.B.Jacobs, J.W. Odendaal, April 18, 2011
- 5) Progress In Electromagnetics Research, R. Dehdasht-Heydari, H.R. Hassani, A.R. Mallahzadeh, PIER 81, 183–195, 2008
- 6) Progress In Electromagnetics Research, R. Dehdasht-Heydari, H.R. Hassani, A.R. Mallahzadeh, PIER 79, 23–38, 2008
- 7) Yin J., Yang J., Pantaleev M. “The Circular Eleven Antenna: A New Decade-Bandwidth Feed Reflector Antennas With High Aperture”, Ieee Transactions on Antennas and Propagation, vol. 61(8), pp. 3676-3984, 2011
- 8) Olsson R., Kildal P.-S., Weinreb S., “The Eleven Antenna: A Compact Low-Profile Decade Bandwidth Dual Polarized Feed for Reflector Antennas”, Ieee Transactions on Antennas and Propagation, vol. 54, no. 2, 2006
- 9) J. Yang, X. Chen, N. Wadefalk, and P.-S. Kildal, “Design and realization of a linearly polarized eleven feed for 1-10 GHz”, IEEE Antennas Wireless Propagation lett., vol. 8, pp 64-68, 2009
- 10) P. Hall, “The square kilometre array: An international engineering perspective”. The Square Kilometre Array: An Engineering Perspective, pp. 5-16, 2005
- 11) Reference manual. QSPCP2-18SRHRA, Circularly polarized Spiral Antenna. Q-par Angus
- 12) Reference manual. Model 4010180, 1-18 GHz 180° hybrid coupler. Krytar
- 13) Y.V.Pimenov, V.I. Volman, A.D. Muravtsov “Technical Electrodinamics”, Moscow, 2002
- 14) High Frequency Materials, products selector guide, 11/2010, Rogers
- 15) Reference manual. Model 1830, 2-18 GHz 90° hybrid coupler. Krytar